Water jets surrounded by an air film

(Experimental research on the influence of air addition around water jets)

M.Sc. Thesis

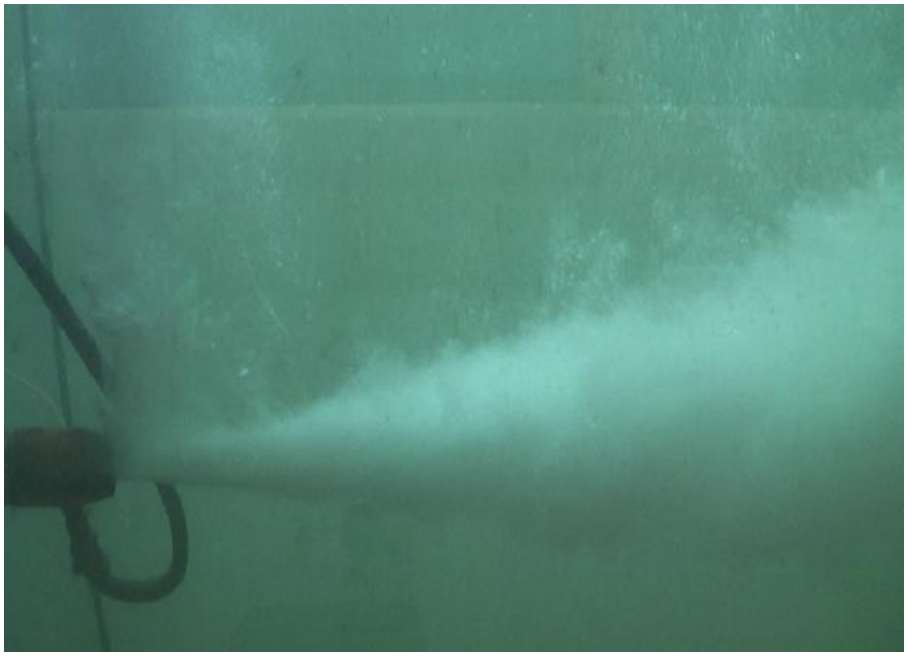

TU Delft
Delft University of Technology

Royal
Boskalis Westminster nv

F.R.S. Vinke

Master:	Hydraulic engineering	CITG
Specialization:	Dredging engineering	CITG

CONFIDENTIAL

2 years

Graduation committee:

prof. dr. ir. C. van Rhee	TU Delft	3ME/CITG
dr. ir. A.M. Talmon	TU Delft	3ME
ir. G.L.M. van der Schrieck	TU Delft	CITG
ir. A.J. Nobel	Boskalis	DDD

During the research some confidential information is applied. In this version of the thesis, that data is removed. For more information the reader is referred to prof. dr. ir. C. van Rhee (TU Delft) or W. Rosenbrand (Boskalis; department DDD).

Preface

This master thesis is an experimental study to the influence of an air film around a water jet. The study has been carried within the curriculum of the faculty Civil Engineering and Geosciences at Delft University of Technology.

In this report the literature study is not included. The literature study is brought together in another report and is a supplement of this report.

During the master thesis I got a lot of help and guidance of a number of people.
First of all, I would like to thank A.J. Nobel as the daily supervisor during the research.
A lot of thanks go also to the other people of my graduation committee for their guidance and comments during this research.

Thanks go to the people of Boskalis that helped me during the design & construction of the supporting frames and build up of the experimental setup in the laboratory of Boskalis.

I would like to thank also the following persons:

- Mr. M. Grootenboer of Deltares for his advice and supply of the measuring probes
- dr. ir. R. Delfos of the laboratory of Areo-and hydromechanics (3ME, TU Delft) for his help with the design of the air discharge meter.
- ir. K. Slager of the dredging development department (DDD) of Boskalis for his assistance during the experiments and his help with the report.
- Margot van Aalderen, my roommate during the research, for her support and the help with the report.

Last, but not least I would like to thank my family and my wife Hanneke for their support.

F.R.S. Vinke

June 2009

Summary

The effect of introducing an air film around a submerged water jet is examined in laboratory experiments. The objective is to reduce the friction forces between the water jet and the ambient fluid, making a jet potentially more effective at a larger distance. The test are conducted at a physical scale comparable to dredging practise, contrary to earlier experiments reported in the literature, where small scale jets are tested. During the tests the development of the jet was measured in axial and radial direction. The jet pressure and air discharge are varied, leading to a number of combinations of jet pressures and air discharges. The results showed that also at this scale the development of the water jet is influenced by the air film, although not as much as in the earlier experiments. Governing parameters have been established. Examples are the volume, mass and momentum ratios between the air flow and water flow.
The ratios of the air flow and water flow are not in the same order if the comparison is made between the large and small scale water jets. Relatively less air was added in the test of a water jet at the scale used in dredging practise.
Adding air around a water jet has a positive effect on the development of a water jet, if enough air is added. With increasing size of the nozzle diameter, more air has to be injected to create an effective air film. If enough air is added to create an effective air film, the effect is observed at very large axial distances.
A description of this type of jets is given based on the description of Yahiro and Yoshida (1974) of water jets surrounded by an air film and the description of Rajaratnam (1976) of submerged water jets.
The total amount of energy of the water jet and air film can also be used to create a water jet without an air film. A water jet without an air film with the same amount of energy does not result in the same velocity increase as observed if an air film is created.

Table of contents

Chapter 1 Introduction

Problem analysis
One of the most important processes in dredging is excavation of soil. This can be done in different ways, e.g. cutting. Another method is the use of water jets. An important aspect for the jetting of soil is the excavation capacity. This capacity is determined by the amount of momentum exposed to the soil.
In most applications the penetration depth of the jet is also important. An example is environmental dredging (Beaudredge, see appendix K). This application uses a water jet rotating in the horizontal plane in the ground to excavate a clean layer of soil beneath a polluted layer or a layer with high ecological value. The advantage of Beaudredge is that the polluted layer or the layer with high ecological value does not have to be removed. The amount of soil excavated within one rotation depends on the penetration depth of the water jet. A larger penetration depth will lead to a higher excavation capacity.
Due to the resistance between the jet and ambient fluid the velocity is reduced. The jet will also pick up small soil particles and water which also cause a decrease of the velocity of the jet. At a certain distance the velocity of the jet is at such a low level that the excavation capacity goes to zero.

Research has been carried out by Ginniken et al (2006) on a water jet with addition of air. These tests showed that the resistance between the water jet and the ambient fluid is reduced by the added air, resulting in less loss of the stagnation pressure in the flow direction. This resulted in a larger penetration of the jet into the ambient fluid. These tests are done on small scales (nozzle diameter of 3 mm) and the question is if the decrease of resistance can also be observed on scales used in dredging practice (nozzle diameter of 3 cm).

Objectives
The tests on small scale air-water jets led to a number of questions. These questions are the motive to start this master thesis. The questions are formulated in a number of objectives.

The objectives of the research are:

- Which method of air injection is most effective; an air film around the water jet or adding air to the water jet at the centre axis[1]?
- Measurement of the development of the velocity profile in axial and radial direction to determine to what distance from the nozzle the air film has influence on the velocity profile.
- Determine the air discharge for the formation of an air film around the jet for different jet pressures and the optimal air discharge.
- Quantification of the thickness of the film of air and the distance where over this air film is present.

[1] The measurements with air addition in the centre of the axis are cancelled, because the experiments couldn't be finished within the time span.

Chapter 2 Hypotheses

In this chapter hypotheses will be presented based on the literature study, Vinke (2009). It is tried to formulate the hypotheses in such a way that most of the parameters in the objectives are quantified. The parameters are the air discharge Q_a, the distance x to the nozzle, the downstream velocities as a function of axial and radial position. The information is used to design the setup of the experiments and to determine the conditions to be tested.

The hypotheses are:

- The length of the potential core, the distance where over the velocity at the centre axis equals the exit velocity of the jet, for a submerged water jet is six nozzle diameters ($6*D_n$), while a length of the potential core is observed between thirty and thirty six nozzle diameters ($30\text{-}36*D_n$) in case of an air-water jet in water on small scale. The length of the potential core will be in the range of 6-36 nozzle diameters.
- The cross-sectional velocity profile has the shape of a Gaussian distribution beyond the potential core. Inside the potential core the cross-sectional velocity profile has a more 'top-hat'-shape.
- A minimum amount of air is required to create an effective air film. For different type of jets the expected air entrainment is given in Table 1. As reference the entrainment of a submerged water jet is considered. The entrainment of air or water, depending on the type of jet, is determined at a distance of 36 nozzle diameters.

Table 1 Entrainment of a number of types of jets

Type	D_n [m]	Q_a [l/s]	
		min	max
Water jet discharging in air	0.003	4	14
Water jet discharging in air	0.03	xxx	xxx
Plunging jet	0.03	xxx	xxx
Reference case		Q_w [l/s]	
		min	max
Submerged water jet	0.03	xxx	xxx

- If a water jet with an air film is considered, the velocities at the centre axis increases with increasing air discharge. For large air discharges the effect on the velocities at the centre axis decreases. Above a certain discharge no effect is observed. So an optimum air discharge exists.

- The important parameters of the velocity development beyond the potential core are:
    1. the nozzle diameter D_n [m]
    2. the exit velocity u_0 [m/s]
    3. the distance to the nozzle x [m]
    4. scaling parameter α [-]

  A description of the development is according Rajaratnam (1976):

$$u_m(x) = \frac{\alpha * D_n * u_0}{x} \tag{2.1}$$

  Depending on the air discharge the parameter α will change. The value of the parameter α is 6.3.

  Another description is an exponential decay of the pressure at the centre axis beyond the potential core. This development is observed if water jets with an air film are considered (Yahiro and Yoshida, 1974).

$$p_m(x) = p_0 * e^{C_1(x-L)^{C_2}} \tag{2.2}$$

With C_1, C_2 = scaling parameters [-]
p_0 = the exit pressure [m/s]
x = the distance to the nozzle [m]
L = length of the initial region [m]

Chapter 3 Setup of the experiment

In this chapter the design and construction of the experimental setup is described. Also the measurement program is given for the tests carried out in the laboratory of Boskalis.

3.1 Dimensions of the components of the setup

The experiments are carried out in the laboratory of Boskalis in Papendrecht in a flume. A schematic overview of the total experimental setup in the flume is given in Figure 1.

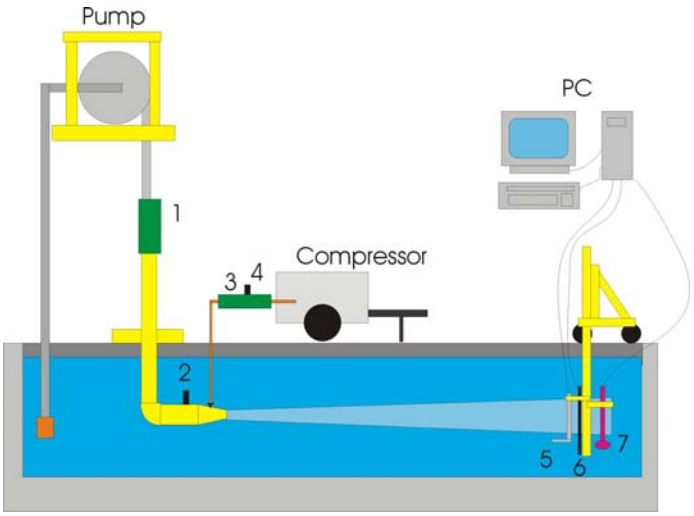

Figure 1 Schematic picture of the setup

In the figure the numbers represents:

1. water discharge meter
2. water jet pressure
3. air discharge meter
4. orifice plate
5. pitot tube
6. array of conductivity probes
7. EMS

An overview of the locations of pump, compressor, discharge meters and support constructions is given in Figure 2. The figure shows also the connections between the separate parts of the experimental setup.

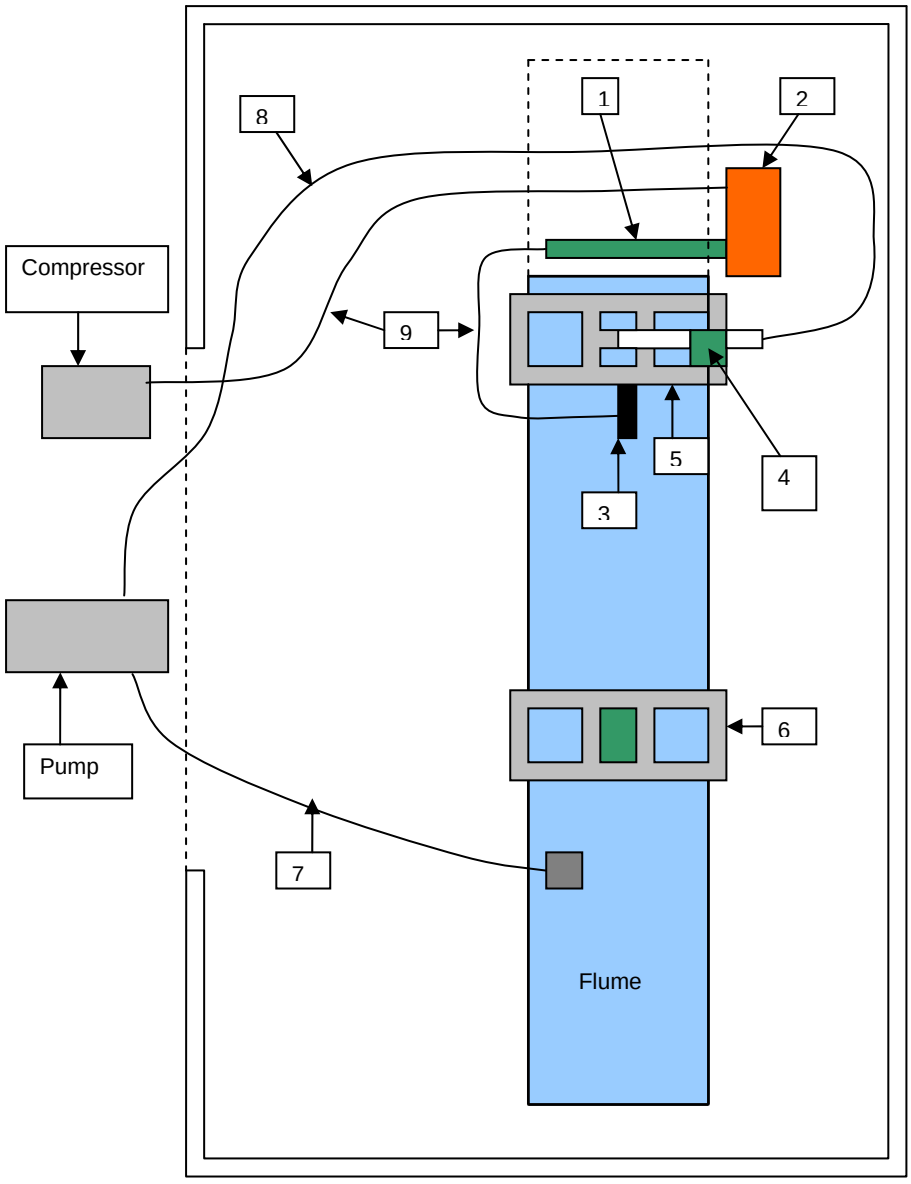

Figure 2 Plan of the setup in the laboratory

1. Discharge meter (air); d_{inner}= 80 mm
2. Pressure vessel; Volume = 60 l
3. Nozzle
4. Discharge meter (water); d_{inner}= 80 mm
5. Fixed construction of the water jet; $d_{pipe;inner}$=80 mm
6. Carriage with measuring probes
7. Hose; length = 12 m and d_{inner} =254 mm
8. Hose; length = 20 m and d_{inner} =80 mm
9. Hose; length = 15 m and d_{inner} =25.4 mm

Flume
The dimensions of the flume are 30 * 2.4 * 2.2 m (L * W * H). In the wall of the flume a window is situated. A schematic picture of the flume is given in Figure 3.

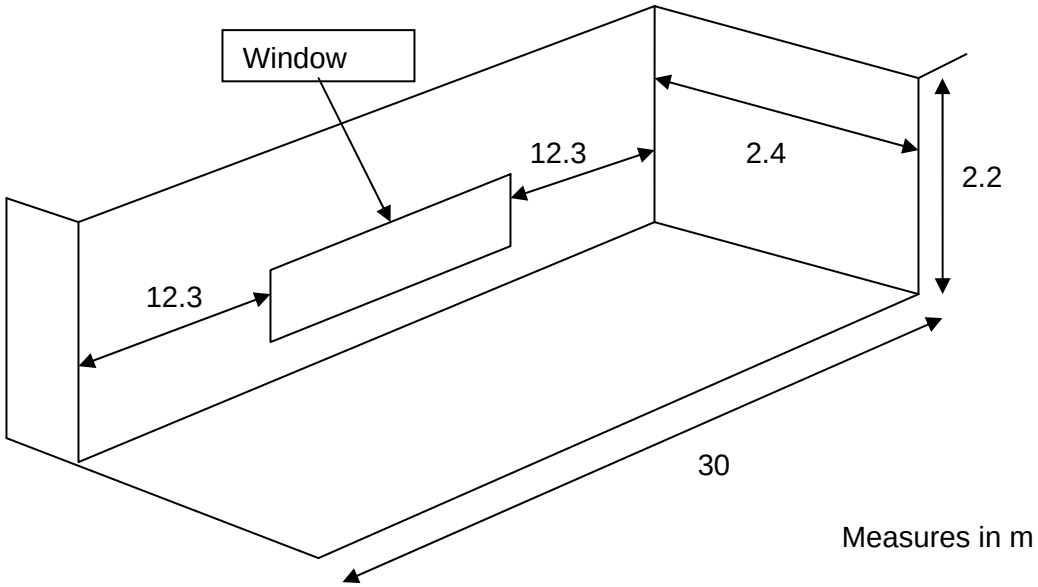

Figure 3 Schematic drawing of the flume

Pump
A range of jet pressures was specified to be tested, leading to the specifications for the jet pump. The jet pressures vary in the range of xxx-xxx bar, such that the jet pressures used in dredging practise (xxx and xxx bar) are included. The lower and higher jet pressures are tested to observe the effect of an air film if different jet pressures are used. The corresponding range of water discharges is 19-33 l/s. The discharges of the pump give the requirements for the water flow discharge meter.

Compressor
From the hypotheses it is concluded that a lot of air has to be added to observe a similar effect as at small scale. A large and expensive compressor is required if these air discharges are added. At the start of the experiments a smaller compressor is chosen. Later on a second compressor is added to the system to investigate whether adding larger amounts of air improves the effect of the air film. Table 2 shows the points of operation of the compressors. The last column of Table 2 shows the maximum air discharges according the air discharge meter for both compressors. The air discharges are determined for atmospheric conditions.

Table 2 Properties of the compressors

Compressor(s)	Point of operation		Q_a [l/s] discharge meter
	p [bar]	Q_a [l/s]	
1	7	83	70
2	7	66	50

The total air discharge Q_a of the compressors together added to the jet is 90 l/s.

Air discharge meter
The specifications of the compressor(s) set the requirements for the air discharge meter. The air discharge meter must be able to measure the air discharges added to the water jet.

The air discharge meter is based on the principle of an orifice plate[2]. The hole in the orifice plate has a diameter of 40 mm. A sketch of the orifice plate is given in Figure 4.

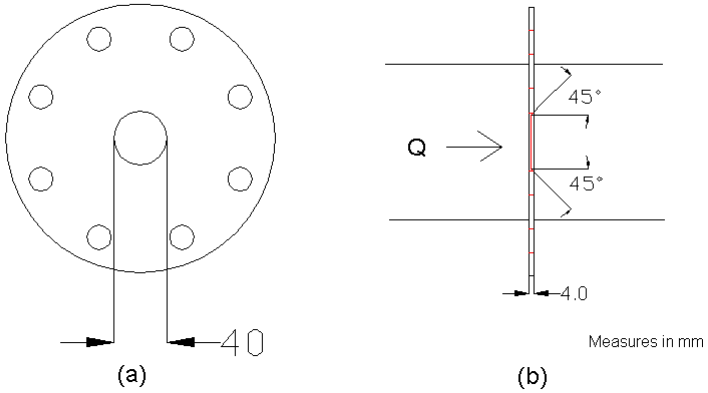

Figure 4 Orifice plate; (a) front view (b) side-view

The pipe has an inner diameter of 80 mm. This measure is a standard size for pipes. For larger diameters of the orifice the pressure difference over the orifice plate becomes small. Very sensitive probes are required to measure the small pressure differences. These probes are not available. If the inner diameter of the pipe is smaller the Mach-number, $Ma = u / u_{sound}$, is such that unwanted effects in the air discharge meter occur.

The pressure and temperature are measured at a distance of one inner diameter upstream of the orifice plate, while the pressure is measured also at a distance of half the inner pipe diameter downstream of the orifice plate. In Figure 5 the locations of the pressures and temperature sensors are shown.

[2] The principle of this method is described in appendix A.

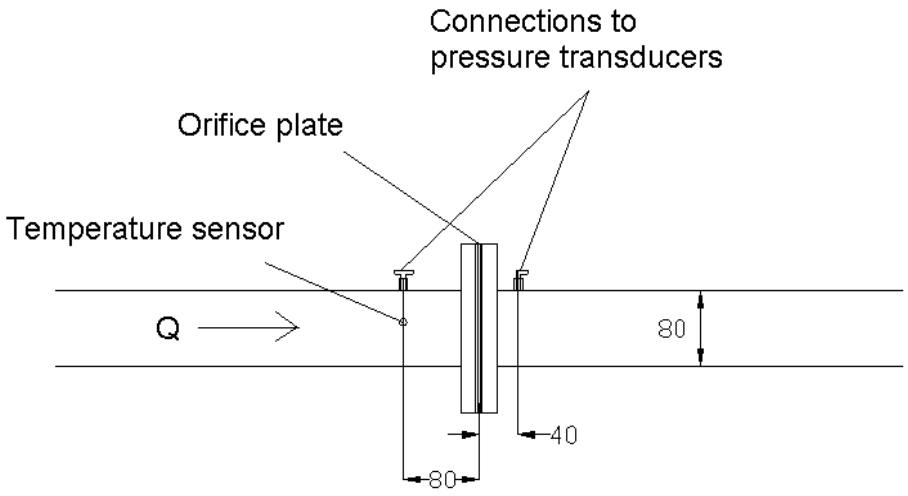

Figure 5 Locations of the pressure transducers and temperature sensor; measures in mm

For technical drawings of the air discharge meter and the separate components, see appendix G.

Water discharge meter

The water flow discharge meter was situated above the fixed construction of the water jet. The discharge meter includes special pipe segments in front and after to ensure steady flow through the discharge meter. See Figure 6.

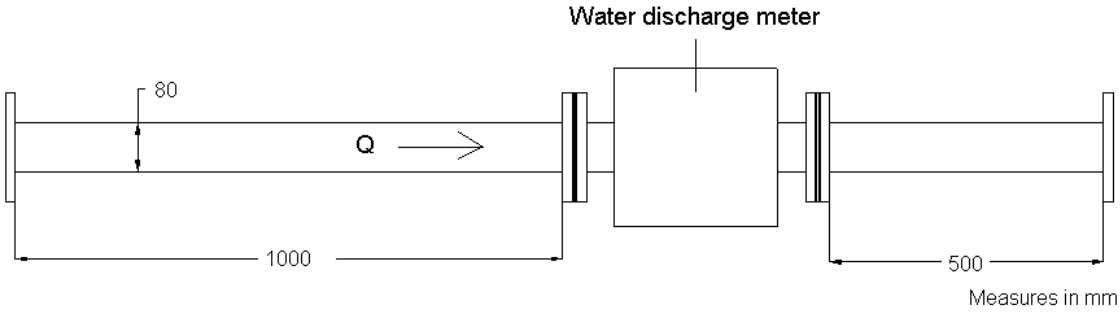

Figure 6 Schematic picture of the water discharge meter

Besides the separate measurement devices, two supporting constructions are used: a fixed support for the water jet and a railway carriage with measurement devices. The technical drawings of these constructions can be found in the appendix G.
In this paragraph schematic figures will be given, including the most important dimensions.

Support of the water jet
The support of the water jet is shown in Figure 7.

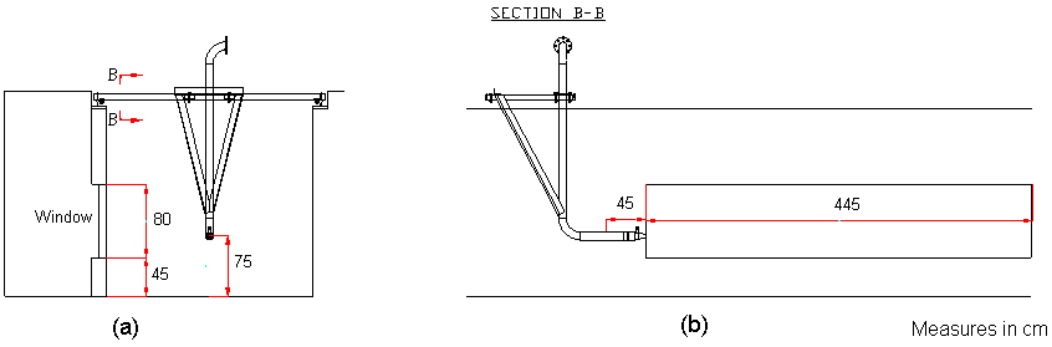

Figure 7 Water jet construction (a) front view (b) side-view

The centre of the jet is positioned 0.75 m above the bottom of the flume. The nozzle is aligned with one of the window ends. The location of the nozzle is chosen such that it is possible to record the jet with a video camera. The camera is located in the room next to the flume. The height of the window is 0.80 m, the width 4.45 m and it is situated 0.45 m above the bottom of the flume.
The water depth in the flume during the tests was 1.80 m. So the jet is positioned 1.05 m under the free water surface. The water depth is chosen such that the influence of the boundaries of the water body on the water jet is minimized.

At a distance of 0.45 m upstream of the nozzle orifice the pressure of the flow was measured. The pressure of the air inlet was measured 7 cm in front of the air chamber. See Figure 8. The positions are chosen such that the pressures are measured close to the nozzle, but outside the influence zone.

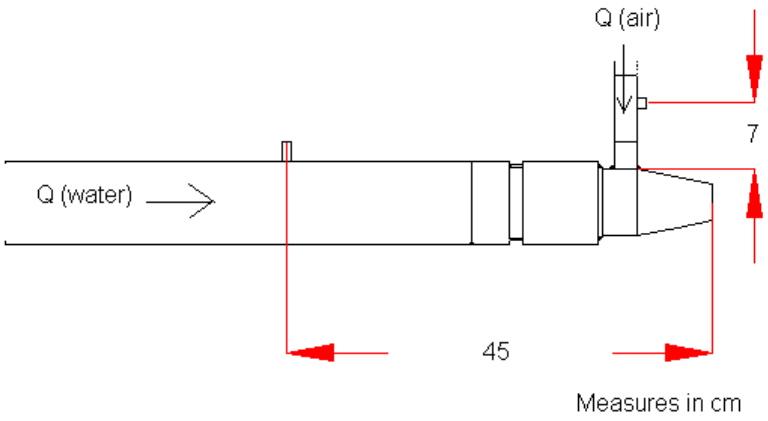

Figure 8 Locations where the pressures are measured.

Nozzle
The specifications of the nozzle are given in Table 3.
The diameter of the nozzle equals the dimension of the nozzles used in dredging practice. The inner diameter of the air chamber is chosen such that the air is brought as close as possible to the water jet. To ensure the loss of pressure is not too large an air slit of 4 mm is chosen. Figure 9 shows the nozzle and air chamber.

Table 3 Overview of the nozzle properties

D_{jet} [mm]	$D_{inner,\ air}$ [mm]	$D_{outer,\ air}$ [mm]	A_{jet} [mm^2]	$A_{airslit}$ [mm^2]
30	36	44	$7*10^{-4}$	$5*10^{-4}$

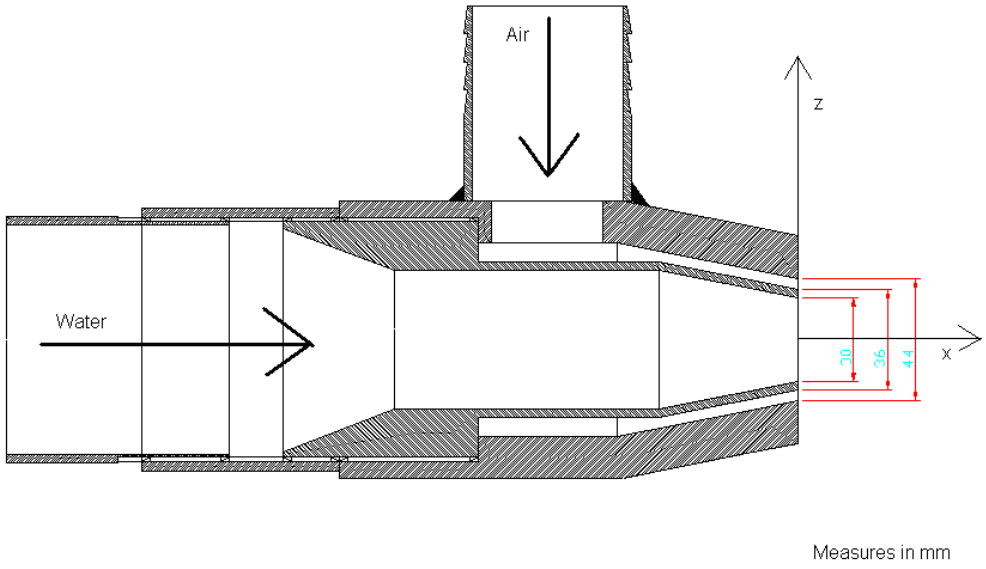

Figure 9 Figure of the nozzle and air chamber, and coordinates

Carriage

The carriage can be translated in x-direction over a railway. A support frame for the measurement devices is attached to the carriage. The frame can be translated in y-and z-direction relative to the carriage. So using this carriage, the measurement devices can be positioned in the x-, y- and z-direction. The used axis system is given in Appendix D. The measurement devices mounted on the frame are the pitot tube, the EMS and the conductivity probes (see Figure 10).

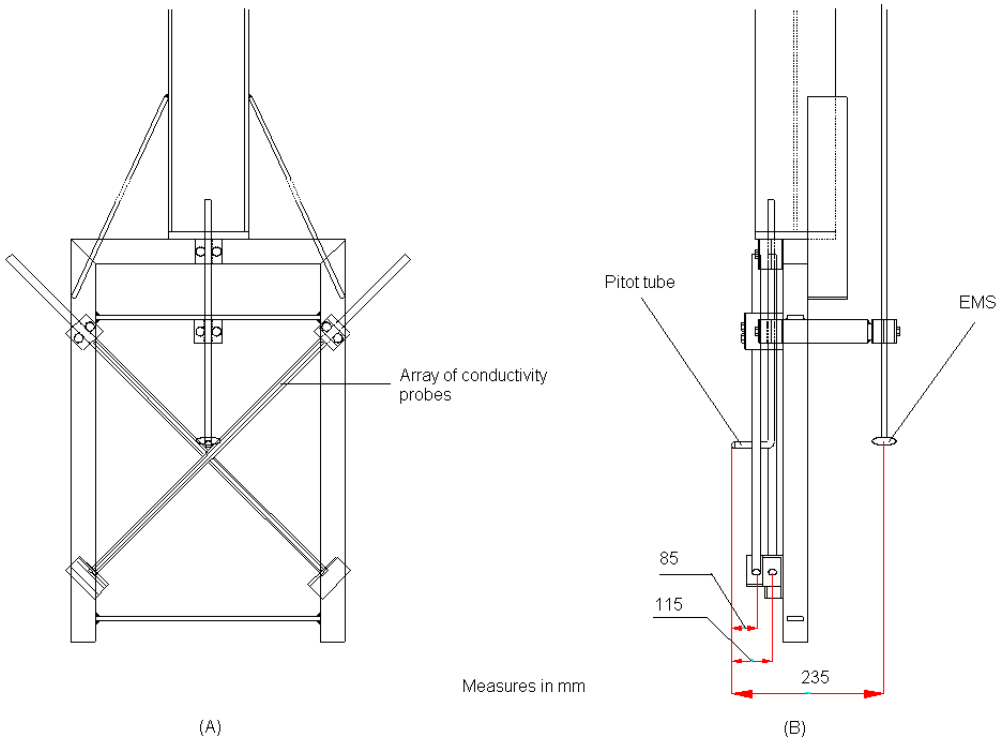

Figure 10 Measurement equipment mounted on frame (A) front view (B) side view

Measuring probes
The probes are placed in such a way that the influence on each other is minimized.

The dimensions of the equipment are:

- Pitot tube:
  In the tests two pitot tubes are used:
  The outer diameters are 8 and 10 mm.
  The diameter of the inlet at the tip of the pitot tube is approximately 3 mm.
- EMS:
  The device measures the velocity in two directions (x- and y-direction).
  Measurement range: $\pm$ 5 m/s.
- Array of conductivity probes (the calibration is given in appendix F):
  Pairs of probes are mounted on a tube with a distance of 40 mm between the pairs

The final design of the different parts of the experimental setup will be given in an overview of pictures in Appendix B.

3.2 Parameters

In paragraph 3.1 already a number of measurement probes are mentioned. In this paragraph a full list of the probes is given. These variables can be obtained from the objectives set in chapter 1, they are:

- Which method of air injection is most effective; an air film around the water jet or adding air to the water jet at the centre axis[3]?
- Measurement of the development of the velocity profile in axial and radial direction to determine to what distance from the nozzle the air film influences the velocity profile.
- Define the air discharge for the formation of an air film around the jet for different jet pressures and the optimal air discharge.
- Quantification of the thickness of the film of air and the distance where over this air film is present.

These goals lead to the most important parameters measured during the experiments:

- Downstream velocities as a function of axial and radial position [m/s]
- Air discharge [l/s]
- Air jet pressure [bar]
- Water jet pressure [bar]
- Water discharge [l/s]
- Distance of the measuring probes to the nozzle [m]

There are a number of methods to measure each parameter and a description of these devices is given in appendix A. For each parameter one device has been chosen. The motivation of the choices of measurement methods is given in appendix A.
For the experiments carried out during this research the pitot tube and EMS are chosen to measure the velocities. The principle of the pitot tube is based on the equation of Bernoulli. In case of a pitot tube the relation for the velocity and the static and dynamic pressure becomes:

$$p_d - p_s = \frac{1}{2} * \rho * u^2 \qquad (3.1)$$

with	p_d =	dynamic pressure	[Pa]
	p_s =	static pressure	[Pa]
	ρ =	density of the air-water mixture	[kg/m3]
	u =	velocity	[m/s]

In this equation the density of the mixture is one of the parameters. The density of the mixture is measured using an array of conductivity probes. The principle of the EMS and the array of conductivity probes are given in appendix A.

For the measurement of the air discharge, a special device was designed and constructed based on an orifice plate. The orifice was designed and constructed by dr. ir. R. Delfos of the laboratory of Areo-and hydromechanics (3ME, TU Delft).
In the air discharge meter the temperature, the static pressure and the pressure difference over the orifice plate are measured to be able to determine the air discharge. The principle of the air discharge meter is described in appendix A.

[3] The measurements with air addition in the centre of the axis are cancelled, because the experiments couldn't be finished within the time span.

An overview of the variables and the devices is given in Table 4.

Table 4 Overview of the signals

Signal	Variable	Equipment	Range	Dimensions
1	jet pressure	pressure transducer	0-xxx (absolute)	[bar]
2	water discharge	discharge meter	0-xxx	[l/s]
3	air temperature	temperature sensor	-25 -100	[degrees Celsius]
4	Δp over orifice plate	pressure transducer	0-xxx(relative)	[kPa]
5	p_{static} in discharge meter	pressure transducer	0-xxx (relative)	[bar]
6	air jet pressure	pressure transducer	0-7 (relative)	[bar]
7	$\Delta p = p_{dyn} - p_{stat}$ of pitot	pitot tube	0-xxx (relative)	[bar]
8	p_{stat}	pitot tube	-xxx/+xxx (relative)	[bar]
9	p_{dyn}	pitot tube	0-xxx bar (absolute)	[bar]
10	velocity	EMS	0-5	[m/s]
11	density	Array of conductivity probes		[kg/m^3]
12	distance	distance meter	0-12	[m]

N.B.1 The atmospheric pressure [mbar] is measured using a barometer. This variable was not logged by the computer program, but registered manually. The variable is necessary, because some of the pressure transducers measure the absolute pressure, so including the atmospheric pressure.

N.B.2 The axial distance of the probes to the nozzle is measured in meters, but in the calculations the axial distance is expressed in a factor times the nozzle diameter and is defined as x/D_n . Herein is x the distance in meters and D_n the nozzle diameter in meters.

The analogue signals of the measuring probes are transferred to digital signals via an AD-convertor. The system used is an Opto-22. This system is able to sample the signals with a frequency of 1-10 Hz.

3.3 Measurement procedure

Before an experiment can be executed and a measurement is recorded a number of steps have to be carried out to adjust the devices to the desired test conditions.

1. Start logging
2. Start camera recording
3. Adjust to wanted jet pressure
4. Adjust to wanted air discharge
5. Place measurement frame at the wanted distance
6. De-aeration of the pressure transducers
7. Find the centre axis of the jet by translating the measurement frame

8. In case of the velocity profiles the vertical or horizontal position is changed

To be able to adjust to the desired water pressures and air discharges two persons are present during most of the tests.

3.4 Test matrix

To be able to get the most relevant information out of the tests in the available time span, it is necessary to set up a test matrix beforehand. The test matrix is constructed via the following procedure.
First the parameters that are varied during the experiments are determined. These parameters are the jet pressure, the air discharge, the radial distance and the axial distances.
Then combinations of these variables are made and the expected theoretical results are plotted in figures. With help of these figures the minimum amount of tests could be determined. The necessary tests are put in a matrix; seeTable 5 to Table 7 of paragraph 3.4.3.

3.4.1 Expectations of a submerged water jet

The submerged water jet without air addition can be described using the formulation of Rajaratnam (1976).

The measurements of water jets without air addition are used as reference to the measurements of the water jets with air addition. It also is a check if the current setup is suitable to measure the water jet.

One of the descriptions given by Rajaratnam (1976) is the development of the velocity at the centre axis of the water jet at downstream axial positions. The distance to the measuring probes is normalized with the nozzle diameter. The measurement positions are multiplications of the length of the potential core. The length of the potential core is approximately six nozzle diameters ($6*D_n$).
The curves according to Rajaratnam (1976) for different jet pressures are shown in Figure 11. The distances are $x/D_n = 6, 12, 24, 36$. If the normalized velocity is plotted versus the axial distance the measurement can be described by:

$$\frac{u_m}{u_0} = \frac{6.3 * D_n}{x}$$

With	u_m	velocity on the centre axis of the jet in radial direction	[m/s]
	u_0	exit velocity	[m/s]
	D_n	nozzle diameter	[m]
	x	position to the nozzle in axial direction	[m]

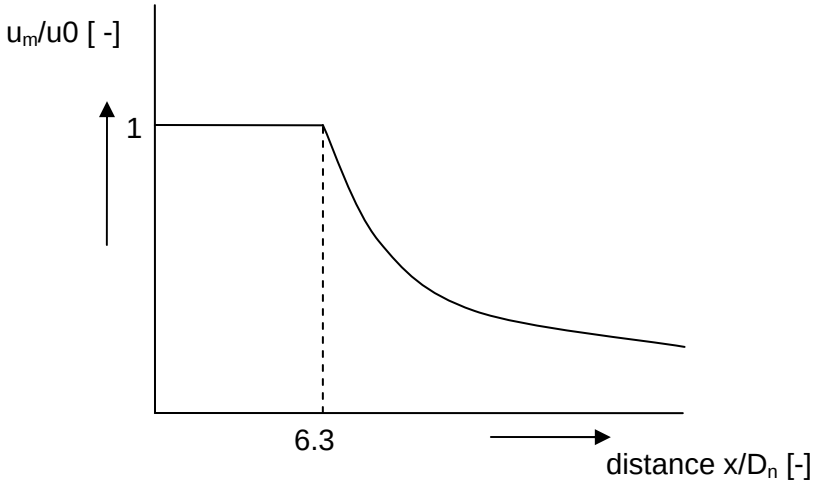

Figure 11 Development of submerged water jets in axial direction.

Rajaratnam (1976) gives also a description for the development of the cross-sectional velocity profile in x-direction. The shape of the profiles is Gaussian. The description is

$$u = u_m * e^{\left(-0.693\left(\frac{R}{b}\right)^2\right)}, \quad b = 0.1x$$

With	u_m	velocity on the centre axis of the jet	[m/s]
	u	velocity in radial direction	[m/s]
	b	width parameter	[m]
	R	radial distance	[m]
	x	position to the nozzle in axial direction	[m]

The velocity will be measured at the centre axis and at a number of points on both sides of the centre axis. To study the development of the velocity profile, the profiles at four distances are measured. The values of these distances are x/D_n = 6, 12, 24 and 36. This is done for one jet pressure: xxx bar. The expected profiles at these positions are plotted in Figure 12.

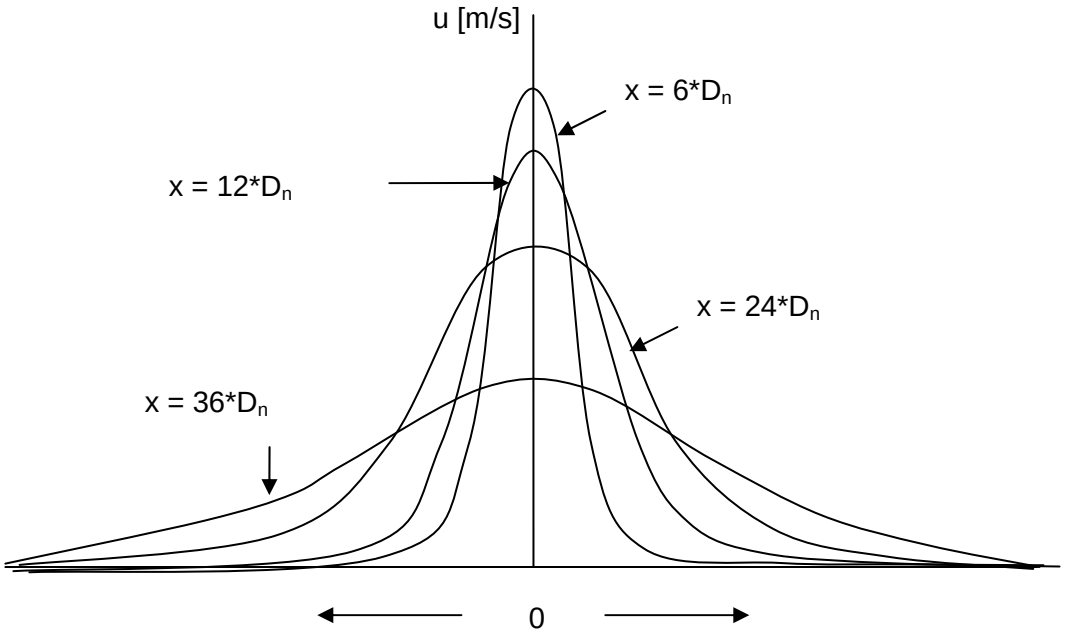

Figure 12 Development of the velocity profile in radial direction

3.4.2 Expectations of a water jet surrounded by film of air

For the jet surrounded with an air film one more parameter is introduced: the air discharge. There are also more combinations of parameters possible.

Figure 13 shows the influence of the air discharge on the velocity at the centre axis for a number of jet pressures at one axial position. An example is at a distance of $x = 24*D_n$.

For small discharges the influence on the velocity is zero or small. Beyond a certain air discharge an increase will be observed. This air discharge is called the minimum air discharge Q_{min}. The increase of the velocity at the centre axis stops beyond a certain air discharge. This discharge is called the optimum discharge Q_{opt}.

The position of the minimum and optimum air discharge depends on the jet pressure. The capacity of a water jet to drag air into a water body is larger if the jet pressure is high. So for low jet pressures a small air discharge is needed to observe an effect on the velocity. The optimum air discharge is also smaller for low jet pressures.

The air discharges will be in the range of 0-84 l/s. The air discharges are given for atmospheric conditions. The jet pressures are between xxx and xxx bar. The velocity was measured at the centre axis at a number distances: $x = 12*D_n$, $24*D_n$ and $36*D_n$. An extra compressor will be installed to be able to inject more air to the jet, in case there is still an increase of the velocity with the maximum air discharge of one compressor.

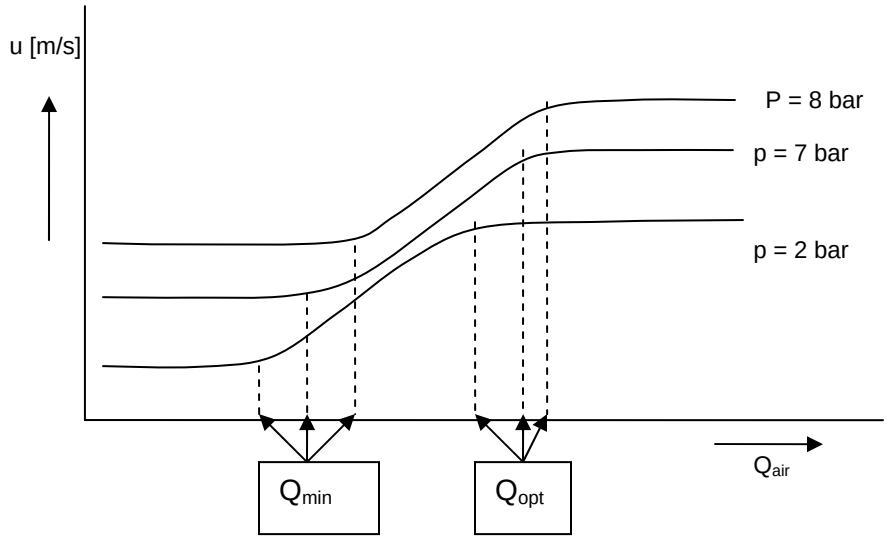

Figure 13 Influence of increase of the air discharge.

The effect of the air film on the cross-sectional velocity profiles is also measured. The cross-sectional velocity profiles are measured at a number of axial distances for a jet with a pressure of xxx bar. The positions where a cross-sectional velocity profile is measured are x = 54*D_n, 72*D_n, 144*D_n and 288*D_n.
Plotting figures of three or four air flow rates the development of the velocity profile can be observed. An example is given in Figure 14. The jet pressure is xxx bar and the air discharges are 16, 50 and 84 l/s, including low, middle and high discharges.

The velocity profile in radial direction (r) for jet with an air film is expected to differ from that of a submerged water jet. One of the differences is that the profile will be more block-shaped as long an air film is present. In the air film the velocity will drop very quickly. For axial distances larger than the potential core the profiles will have the shape of a Gaussian distribution. An overview is given in Figure 14.

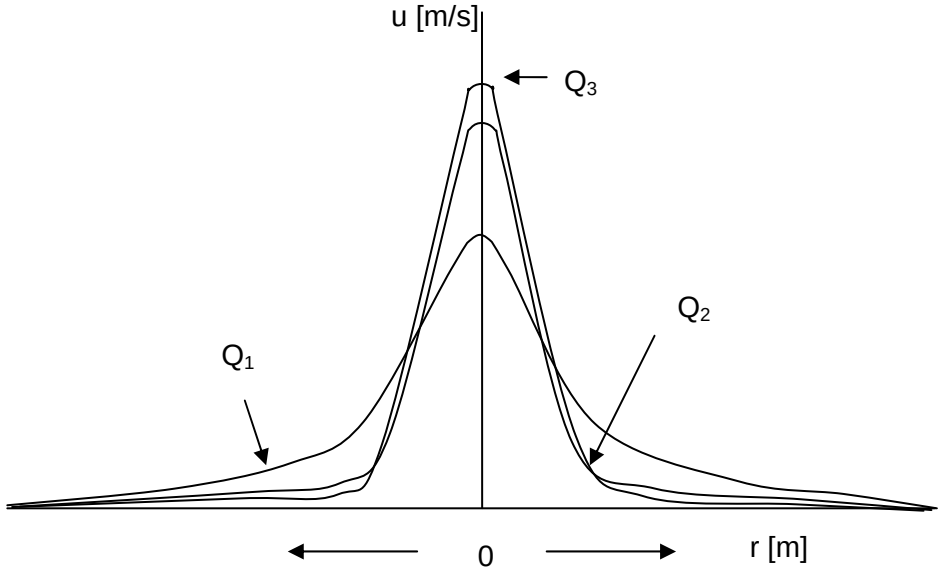

Figure 14 Influence of air discharge on the velocity profile at a certain axial distance.

If an air film is created around the water jet the potential core will increase, according Ginniken et al (2006). The velocities at the centre axis beyond the potential core will increase with increasing air discharge. The air discharges vary in the range of 0-84 l/s. The velocity at the centre axis is measured at a number of axial distances.
The expected influence of the air discharge on the potential core is given in Figure 15.

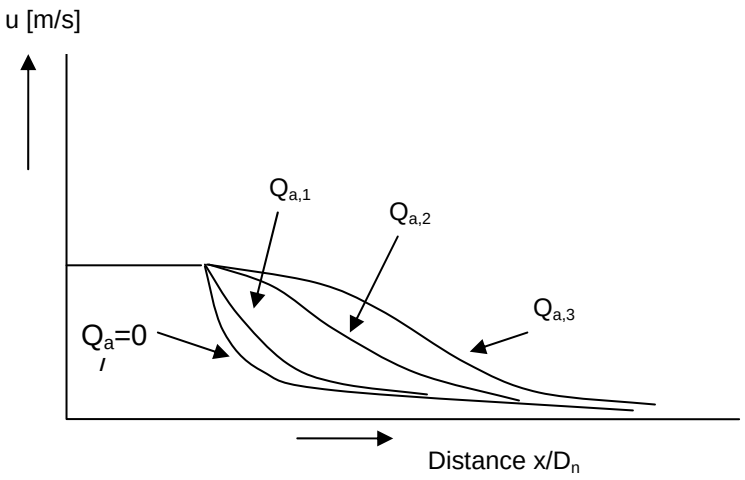

Figure 15 Influence of air discharge on the potential core.

Approximately the same figures can be given if a different suction length is used, or if a different method air injection method is applied.

3.4.3 Test program presented in a test matrixTable 5 and Table 7 show the test program for a submerged water jet and an air-water jet in water. The measurements to examine the influence of the suction length and the type of air addition[4] are included. The suction length is defined as the distance where over the jet is able to entrain air inside the nozzle. This distance is created if the outer nozzle is shifted over a certain distance in axial direction in comparison to the inner nozzle (see appendix G in the technical drawing of the nozzle).

In the tables the following measurement positions are mentioned:
centre = measurement of the velocity only at the centre axis of the water jet
profile = measurement of the horizontal and vertical velocity profile

Table 5 Measurements for a submerged water jet

	x/D_n [-]			
p_{jet} [bar]	6	12	24	36
xxx	*centre**	*centre*	*centre*	*centre*
xxx	centre	centre	centre	centre
xxx	centre	centre	centre	centre
xxx	profile	profile	profile	profile

* In Table 5 to Table 7 the italic printed measurement points are not carried out

[4] These measurements are cancelled, because the experiments couldn't be finished within the time span.

Table 6 Measurements for a water jet surrounded by an air film

										x/D_n [-]					
p_{jet} [bar]	$Q_{air;atmos}$ [l/s]					Suction Length [cm]				24	36	54	72	144	288
	16	33	50	67	84	0	1	2	3						
xxx	*x*	*x*	*x*	*x*	*x*							*centre*			
xxx	x	x	x	x	X							centre			
xxx	x	x	x	x	x							centre			
xxx	*x*		*x*		*x*							*profile*	*profile*	*profile*	*profile*
xxx					*x*		*x*	*x*	*x*	*centre*	*centre*	*centre*	*centre*	*centre*	*centre*
xxx	*x*		*x*		*x*	*x*	*x*	*x*	*x*			*centre*			
xx					*x*	*x*	*x*					*profile*	*profile*	*profile*	

Table 7 Measurements for a water jet with air addition at the centre axis

						x/D_n [-]				
p_{jet} [bar]	$Q_{air;atmos}$ [l/s]					6	12	24	36	54
	16	33	50	67	84					
xxx	*x*	*x*	*x*	*x*	*x*		*centre*			
xxx	x	x	x	x	x		centre			
xxx	x	x	x	x	x					
xxx	x		x		x		profile	profile	profile	
xxx	x		x		x	centre	centre	centre	centre	centre

Chapter 4 Data analysis

The results of the experiments are presented in this chapter. First an overview of the measurements carried out is given. Then the results of the water jets without air addition are discussed. After the water jets without air the effect of air on the development of water jets surrounded by an air film are presented for the different variables; axial distance, air discharge, velocity profile and density. The last paragraph contains the conclusions.

4.1 Overview of the measurements

In Table 8 to
In Table 13 the marks are the positions where the velocity profile in horizontal and vertical direction is measured. The measurements are carried out for three air discharges and a jet pressure of x bar.
Table 13 the measurements actually carried out during the research are presented. This table differs from the table of the planned measurements in the last paragraph of chapter 3. This is because during the tests some adjustments are carried out to the initially planned measurements. The velocities shown in the plots in this chapter are measured with use of the pitot tube. Although an EMS was mounted on the measurement frame no results of this probe are given in the analysis. The range of the EMS was small in comparison to the range of the velocities of the jet. In the range of velocities where the EMS could be applied, the measurements did not give useful results.

In Table 8 to Table 12 the marks are the measurements for the given jet pressure (caption of the table), the axial distance and the air discharge added to the water jet.

Table 8 Experiments carried out with jet pressure xxx bar

p_{jet} = xxx bar	x/D_n [-]									
Q_{air} [l/s]	6	8	10	12	14	16	24	36	54	72
0										
10										
20				x			x	x		
30										
40				x			x	x		
50										
60				x			x	x		
70				x			x	x		
80				x			x	x		
90				x			x	x		

Table 9 Experiments carried out with jet pressure xxx bar

p_{jet} = xxx bar	x/D_n [-]									
Q_{air} [l/s]	6	8	10	12	14	16	24	36	54	72
0	x	x	x	x			x	x	x	x
10				x			x	x		
20		x	x	x	x	x	x	x	x	x
30				x			x	x		
40		x	x	x	x	x	x	x	x	x
50				x			x	x		
60				x			x	x		
70		x	x	x	x	x	x	x	x	x
80										
90										

Table 10 Experiments carried out with jet pressure xxx bar

p_{jet} = xxx bar	x/D_n [-]									
Q_{air} [l/s]	6	8	10	12	14	16	24	36	54	72
0	x	x	x	x	x	x	x	x	x	x
10							x	x		
20		x	x	x	x	x	x	x	x	x
30							x	x		
40		x	x	x	x	x	x	x	x	x
50							x	x		
60							x	x		
70		x	x	x	x	x	x	x	x	x
80							x	x		
90							x	x		

Table 11 Experiments carried out with jet pressure xxx bar

p_{jet} = xxx bar	x/D_n [-]									
Q_{air} [l/s]	6	8	10	12	14	16	24	36	54	72
0	x	x	x	x	x	x	x	x	x	x
10				x			x	x		
20		x	x	x	x	x	x	x	x	x
30				x			x	x		
40		x	x	x	x	x	x	x	x	x
50				x			x	x		
60				x			x	x		
70		x	x	x	x	x	x	x	x	x
80				x			x	x		
90				x			x	x		

Table 12 Experiments carried out with jet pressure xxx bar

p_{jet} =	x/D_n [-]

xxx bar										
Q_{air} [l/s]	6	8	10	12	14	16	24	36	54	72
0	x	x	x	x	x	x	x	x	x	x
10				x			x	x		
20				x			x	x		
30				x			x	x		
40				x			x	x		
50				x			x	x		
60				x			x	x		
70	x	x	x	x	x	x	x	x	x	x
80				x			x	x		
90				x			x	x		

In Table 13 the marks are the positions where the velocity profile in horizontal and vertical direction is measured. The measurements are carried out for three air discharges and a jet pressure of x bar.

Table 13 Experiments carried out for the cross-sectional velocity profiles

p_{jet}= xxx bar	x/D_n [-]			
Q_{air} [l/s]	8	12	24	36
0			x	
35		x		
70	x	x	x	x

4.2 Water jet without air

The measurement of the submerged water jet without an air film is the reference for the measurement of a water jet with air addition. The development of submerged water jet without air is indicated by Rajaratnam (1976).

Figure 16 shows the measured values and the theoretical curves for a number of water jets without air. The jet pressure varies between xxx and x bar. For all jet pressures the measurements fit the theoretical curves.

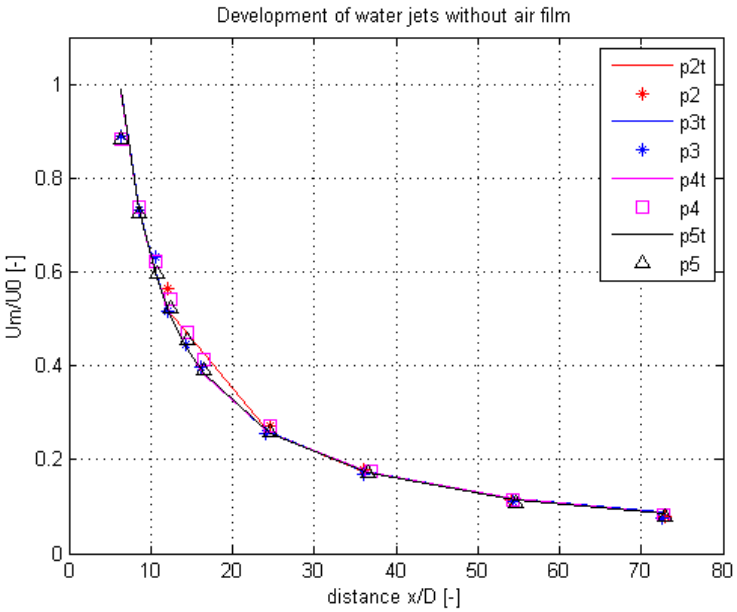

Figure 16 Development of water jets without an air film

The cross-sectional velocity profiles, horizontal and vertical, are measured in case of a water jet with jet pressure xxx bar at a distance of x/D_n =24.
As observed from Figure 17 the measured cross-sectional velocity profiles almost fit the theoretical profiles according Rajaratnam (1976). The small difference might be explained by the fact the water jet is cavitating, which could not be verified.

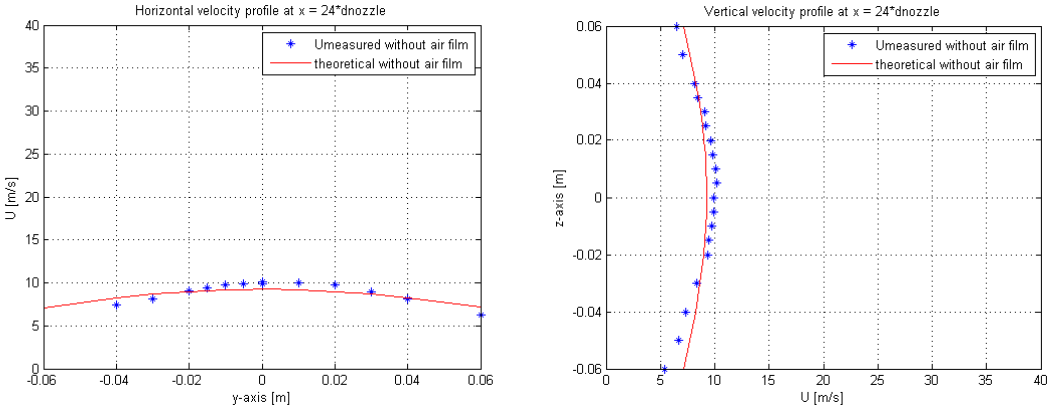

Figure 17 Horizontal en vertical velocity profile at a distance of x = 24*D_n

The current setup of the experiment is able to reproduce the results of previous experiments if a submerged water jet without air is considered, especially if the velocities at the centre axis are considered. In case of the horizontal and vertical velocity profile a difference is observed. No test is carried out to examine if the experimental setup reproduces a water jet surrounded by air only.

4.3 Water jets surrounded by an air film

This paragraph has been removed, because of the confidential information.

Chapter 5 Analysis

The results of the measurements carried out during this research differ from what was expected based on the result of measurements carried out by other researchers with jets at a smaller scale. The current data show a small improvement in a specific range of the axial distance, but this improvement is less than the improvement seen in the data of small scale jets. In the small scale tests an increase of the potential core was observed, while this was not the case during the tests of this research.
A thorough explanation of the differences in improvement is not available yet, but in this chapter some reflections will be given on the possible explanations. First the flow characteristics of the water and air flow will be considered. Than the entrainment capacity of a water jet will be discussed. In the third paragraph the length scale of turbulent eddies in comparison with the thickness of the air film is considered.
Finally the results of the tests are compared to other datasets.

5.1 Flow characteristics.

The first idea is to consider the flow characteristics of air and water. The following characteristics will be examined:

Discharge:

$$Q_0 = u_0 A_0 \tag{5.1}$$

Massflow:

$$\dot{m}_0 = \rho u_0 A_0 \tag{5.2}$$

Momentum:

$$M_0 = \rho u_0^{\,2} A_0 \tag{5.3}$$

Reynolds number:

$$\mathrm{Re} = \frac{u_0 * D_j}{\nu} \tag{5.4}$$

Weber number:

$$We = \frac{u_0^{\,2} * D_j * \rho}{\sigma} \tag{5.5}$$

Thickness of the air film:

$$t = \frac{Q_a}{u_{0;water} * \pi D_j} \tag{5.6}$$

The assumption is that the velocity of the air film equals that of the water jet.

wherein	u_0	=	velocity	[m/s]
	Q_0	=	discharge	[l/s]
	Q_a	=	air discharge	[l/s]
	A_0	=	surface	[m^2]
	ρ	=	density	[kg/m^3]
	m_0	=	mass flow	[kg/s]
	M_0	=	momentum	[N]
	D_j	=	jet diameter	[m]
	t	=	air film thickness	[m]
	$u_{0;water}$	=	exit velocity of the water jet	[m/s]
	ν	=	kinematic viscosity	[m^2/s]
	σ	=	surface tension	[N/m]

Other dimensionless parameters are t/D_n and $t/t_{airslit}$.

The ratio of air over water of these parameters will be determined for various conditions. The maximum and minimum values are given Table 14.

Table 14 Minimum and maximum values of a number of parameters

	Vinke		Ginniken	
	min	max	min	max
Q_{water} [l/s]	xxx	xxx	0.4	1.5
Q_{air} [l/s]	3	54	0.8	7.4
Q_{air}/Q_{water}	xxx	xxx	0.55	17.21
m_{air}/m_{water}	xxx	xxx	$7.17*10^{-4}$	$2.24*10^{-1}$
M_{air}/M_{water}	xxx	xxx	$1.11*10^{-4}$	$1.08*10^{-1}$
Re_w	xxx	xxx	$1.3*10^5$	$4.6*10^5$
We_w	xxx	xxx	$1.3*10^5$	$1.7*10^6$
t [m]	0.001	0.016	0.001	0.014
t/D_n	0.033	0.53	0.33	4.67
$t/t_{airslit}$	0.25	4	2	28

The order of the minimum values is equal of the dimensionless parameters for both situations, while the order of the maximum values differs. The values of the data of Ginniken et al are one or two orders higher. The absolute thickness of the air film is equal in both sets of experiments. Ginniken et al have added relatively more air to the water jet.

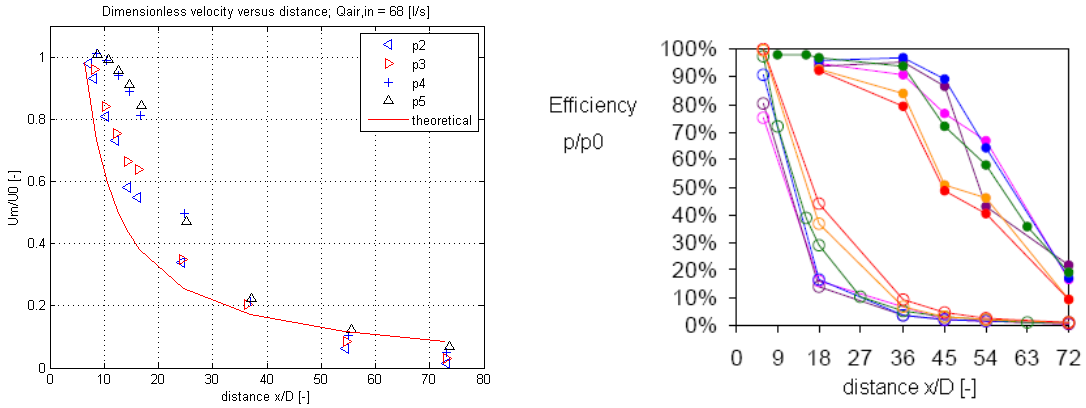

(A) (B)

Figure 18 Axial development of water jets surrounded by an air film (A) Vinke (B) Ginniken

5.2 Entrainment of a water jet.

In the previous paragraph the important parameter is the amount of air that is added to the jet. Table 14 shows that relatively less air is added to the water jets at the scale of dredging practice. In this paragraph a comparison is made between the amount of air added to the jet and the entrainment of a jet.

A ratio $\frac{Q_a}{Q_e}$ is defined, wherein Q_a is the air discharge added to the water jet and Q_e is the entrainment of a water jet.

The entrainment capacity is determined for two types of jets:

1. a submerged water jet
2. a water jet discharging into the atmosphere.

The calculations of the entrainment capacities are given in appendix J.
The outcomes of the calculations are given in Table 15.
The air discharges added to the water jets in the current research are smaller than the entrainment, while in the previous research at smaller scale the range of the applied air discharges is covering the entrainment range mostly.
So in this research adding the theoretical necessary amount of air has not been realized, contrary to the research of Ginniken et al (2006). For a number of combinations Ginniken et al have added more air than the entrainment.

The conclusion is that the effect of an air film is larger if the added air discharge covers a large part of the entrainment.

Table 15 Overview of the entrainment of a number of jets over a distance of 36*D_n.

	D_n = 0.03 m		D_n = 0.003 m	
	min	max	min	max
p_{jet} [bar]	xxx	xxx	16	200
Q_e [l/s] for a submerged water jet	xxx	xxx	4.2	15
Q_e [l/s] [5] for a jet discharging into the atmosphere	xxx	xxx	4	14
Q_{air} during the tests [l/s]	3	70	1	8
Q_{air}/Q_e submerged water jet	xxx	xxx	0.005	1.9
Q_{air}/Q_e jet discharging into the atmosphere	xxx	xxx	0.07	2

5.3 Turbulent length scales and surface roughness

In this paragraph the focus is on the thickness of an air film. The addition of air is not effective if an air film is absent. The thickness of the air film is compared to the disturbances at the surface of the water jet and the turbulent length scales in the jet. If the turbulent fluctuations and the disturbances are large in comparison to the air film thickness, the fluctuations and disturbance can penetrate through the air film. This will lead to contact between the water jet and the ambient fluid and consequently to loss of momentum.

The velocity of the air is assumed to be equal to water jet exit velocity. The thickness of the air film t is calculated by dividing the air discharge by the water exit velocity and circumference, see equation 5.6.

The turbulent fluctuations are present inside the water jet. Occasionally, the turbulent fluctuations penetrate through the air film.
According to Tennekes and Lumley (1972) in a water jet one velocity scale is identified. This is velocity scale is the cross-stream variation of the mean velocity component in x direction U_s. It is defined as the maximum value of $|U_0 - U|$. If jets are considered the scale of the mean flow in x-direction U_0 of the ambient fluid is zero and U is the velocity of the jet. For a jet U_s is the maximum value of U. The maximum velocity at a cross-section is found at the centre axis. So U_s is the velocity at the centre axis.
A cross-stream scale l is defined as the distance from the centre line at which $U - U_0$ is about $U_s/2$. For a jet it was said U_0 =0, so the scale l_t becomes the distance from the centre line at the point where $U = U_s/2$. The result is: l_t equals the parameter b, the distance from the centre line where $U = U_m/2$ if the cross-sectional velocity profile of a jet is considered. U_m is defined as the velocity at the centre axis of the jet. The relation between the turbulent length scales in radial direction l_t and the turbulent length scales

[5] The calculated air discharge is based on the information in the article of Rajaratnam (1998).

in axial direction L_t is analogous to the relation between the parameter b and x, where x is the distance to the nozzle.

The authors of the book indicate that l_t / L_t is constant and is in the order of $6*10^{-2}$.
At position of $x/D_n=36$ the length scale of turbulent fluctuations are determined. The length scale L_t, the length scale of the turbulent fluctuations in axial direction, is changed to the x, the distance to the nozzle. This is done because the analogy between the ratio b/x and l_t / L_t. The results are given in

Table 16.

At the surface of the water jet discharging into the atmosphere also disturbances are present. The dimensions of these disturbances are according to McKeogh et al (1981):

$$\frac{2\varepsilon}{D_n} = 5.98 * 10^{-3} \left(\frac{x}{D_n} \right)^{0.9} \tag{5.11}$$

With

ε	=	dimension of the surface disturbance	[m]
D_n	=	nozzle diameter	[m]
x	=	distance to the nozzle	[m]

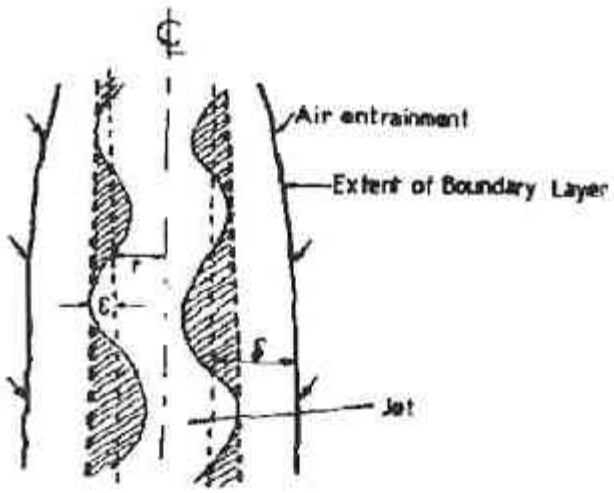

Figure 19 Surface disturbances on jet surface (McKeoch & Ervine, 1981)

Table 16 An overview of the thickness of the air film, the length scale of the turbulent fluctuations and the dimensions of the surface disturbances.

	Vinke		Ginniken et al	
	min	max	min	max
t [m]	0.001	0.016	0.001	0.014
l [m] at x=36*D_n	0.065		0.0065	
t/l	0.015	0.246	0.15	2.15
2ε [m] at x=36*D_n	0.0045		0.00045	
$t/2\varepsilon$	0.22	3.5	2.22	31.1

The ratios between the air film thickness and the turbulent fluctuations and the surface disturbances are one order higher for the smaller jets.

Another approach is to determine the axial distance where the turbulent fluctuations l are of the order of the air film thickness t. An overview of the axial distances is given in Table 17.

Table 17 Positions where length scale of turbulence equals the thickness of the air film

	Vinke		Ginniken	
	min	max	min	max
Distance x/D_n [-]	0.55	8.88	5.55	77.77

At that scale of dredging practise, the turbulent fluctuations are able to penetrate through the air film at smaller axial distance. Due to the absence of an air film the friction between the water jet and the ambient fluid increases.

In **Error! Reference source not found.** the cross-sectional density profiles show an air film up to a distance of 12*D_n. In the tests the water jet was surrounded by a large cloud of air, no clear air film was present (see Figure 49).

5.4 Dataset of Yahiro and Yoshida (1974)

In a later stage the dataset of Yahiro and Yoshida (1974) appeared to be also interesting. They have carried out research on water jets surrounded by an air film. This resulted in a dataset that can be used in the analysis. The characteristics of the water jet and air discharge are given in Table 18.

Table 18 Test conditions of the jet of Yahiro and Yoshida

D_n [mm]	2
p_{jet} [bar]	260
Q_{air} [m^3/min]	0-5
$D_{i,air}$ [mm]	14
$D_{o,air}$ [mm]	16

The dataset used is that of a water jet with a jet pressure of 260 bar and a nozzle diameter of 0.002 m. The air slit is 1 mm and is situated 6 mm outside the water jet in radial direction. The range of the air discharge is 0-5 m^3/min.
In Figure 20 the velocity development at the centre axis of two jets without air are plotted. The jet pressures of the jets are approximately equal. The figure shows that a difference between the velocity developments of the jets exists if no air is added. Although the jet pressure of the jet of Ginniken et al is larger, the velocities in axial direction are smaller. No good explanation for this difference can be given.
As a result a comparison between the two data sets is not allowed.

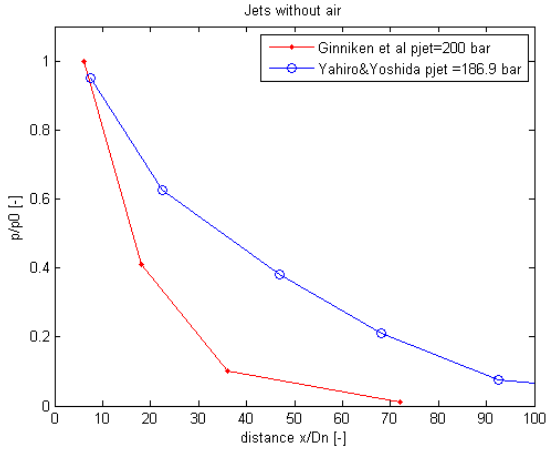

Figure 20 Velocity development at the centre axis for jets without air.

Although the dataset of Yahiro and Yoshida can not be compared with the data sets of Ginniken et al and Vinke, the data set does show the effect of large $Q_{air,in}/Q_{water}$ –ratios. The data set of Yoshida and Yahiro with the specifications of Table 18 is plotted in Figure 21. In the data set higher $Q_{air,in}/Q_{water}$ –ratios are included than used in the data sets of Ginniken et al and the current research.
As seen in the figure the effect of the air film depends on the ratio $Q_{air,in}/Q_{water}$. The effect of the air film on the velocities is observed at larger sand off distances, with increasing $Q_{air,in}/Q_{water}$ -ratio. If the ratio $Q_{air,in}/Q_{water} \approx 100$ an effect is observed up to a distance of x/D_n=300.

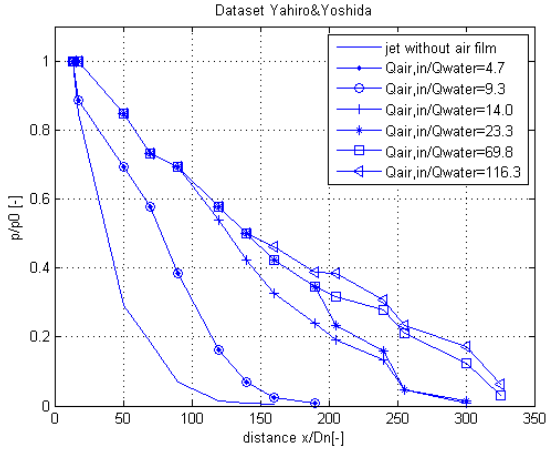

Figure 21 Effect on the velocities with increasing ratio $Q_{air,in}/Q_{water}$

Chapter 6 Description of the a water jet surrounded by an air film

In this chapter it is tried to set up a description of the development of the water jet surrounded by an air film. In previous research a number of descriptions for development of different type of jets have been given.

The description of the development of a submerged jet is according to Rajaratnam (1976):

$$u_m(x) = \frac{\alpha * D_n * u_0}{x} \tag{6.1}$$

Formula 7.1 is translated in to formula 7.2, such the formula is expressed in pressures.

$$p_{stag,m} = \alpha^2 * \left(\frac{D_n}{x} \right)^2 * p_0 \tag{6.2}$$

with

D_n	=	nozzle diameter	[m]
p_0	=	jet pressure	[Pa]
x	=	distance to the nozzle	[m]
$u_m(x)$	=	velocity at distance x at the centre axis	[m/s]
u_0	=	exit velocity	[m/s]
α	=	scaling parameter	[-]

Yahiro and Yoshida (1974) apply to their data set of water jets surrounded by an air film the description:

$$p_{stag} = p_0 * e^{C_1 (x-L)^{C_2}} \tag{6.3}$$

with

C_1, C_2	=	scaling parameters	[-]
p_{stag}, m	=	stagnant pressure at the centre axis	[Pa]
p_0	=	jet pressure	[Pa]
L	=	length of the initial region	[m]

According to Rajaratnam (1976), if a submerged water jet is considered α = 6.3. The length of the initial region is assumed to be 6.3 nozzle diameters.

In the ideal case the air film separates the water jet from the ambient fluid. The potential core would increase and the description of Rajaratnam can be applied from the position

where the air film has broken up in a lot of air bubbles. So in that case the description of Rajaratnam only requires a certain shift c. The description then becomes:

$$u_m(x) = \frac{\alpha * u_0}{x / D_n - c} \qquad (6.4)$$

In reality this is not the case and the data could not described by the eq. 6.4. Just beyond a certain axial distance the description was applicable. The axial distance of 24 nozzle diameters is chosen, because from this distance no air film is observed. So from this position the effect of an air film has disappeared and from this position the description of a submerged water jet can be applied with a certain shift c.

In the domain of 6-24*D_n an other description is used. This region can be described by eq. 6.3. The domain in axial direction is divided in two regions for which one of the descriptions is applied:

$6.3 \leq x/D_n < 24$ Equation 6.3

$24 \leq x/D_n$ Equation 6.4

In Figure 22 the result of is given if the jet pressure is xxx bar and the air discharge is 68 l/s. The shift of the theoretical description of a submerged jet is 11 nozzle diameters.

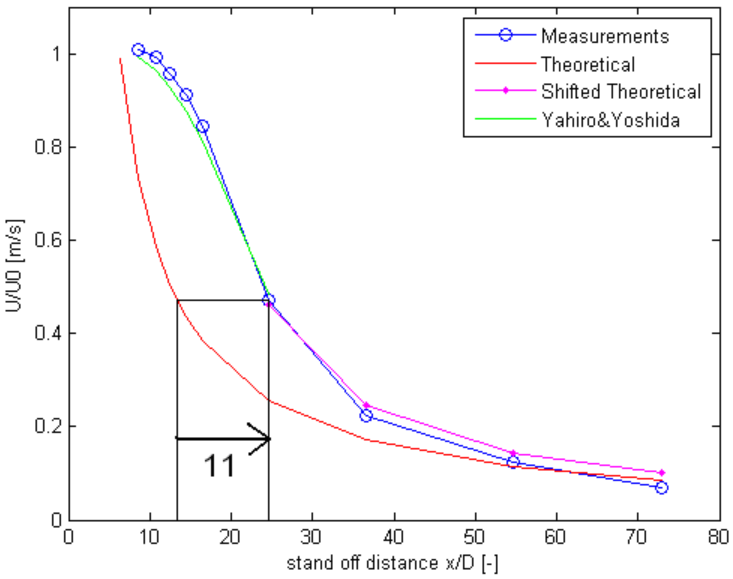

Figure 22 Description of the measurements; p_{jet}=xxx bar and Q_{air} = 68 l/s

In Table 19 an overview of the scaling parameters C_1 and C_2 is given. The table shows a decrease of C_1 and an increase of C_2 with increasing jet pressure. The distance c where over the description of Rajaratnam is translated increases with increasing jet pressure.

Table 19 Overview of the scaling parameters

p_{jet} [bar]	Q_a [l/s]	Q_a/Q_w	C_1 [-]	C_2 [-]	c / D_n [-]
xxx	14	xxx	-0.05	1.2	1
	35	xxx	-0.05	1.06	4
	68	xxx	-0.05	1.05	5
xxx	14	xxx	-0.02	1.6	1
	35	xxx	-0.02	1.4	4
	68	xxx	-0.02	1.35	5
xxx	14	xxx	-0.003	2.3	4
	35	xxx	-0.002	2.15	8
	68	xxx	-0.004	2	12
xxx	68	xxx	-0.0016	2.1	11

The description of the cross-sectional velocity profile is based on a Gaussian distribution indicated by Rajaratnam:

$$u(r) = u_m * e^{a\left(r/b\right)^2} \tag{6.5}$$

with

u	=	velocity	[m/s]
u_m	=	velocity at the centre axis	[m/s]
a	=	scaling parameter	[-]
r	=	radial position	[m]
b	=	radial position to the centre of the jet, where $u/u_m = 1/2$	[m]

The modeling of the cross-sectional velocity profile is tested for a combination of a xxx bar jet and 68 l/s at the axial positions of x/D_n =8, 12, 24 and 38.
In Figure 23 the plots of the cross-sectional velocity profiles are given if the scaling parameter a =-4.5. The value of a gives the best fit with the measurements.
The parameter b is taken as $0.1 * x$. This corresponds with the parameter b for a submerged water jet.

At the position of eight nozzle diameters there is a difference close to the centre axis. The measurements show a wider top than the model. It looks like a ‘top-hat’. This is a cross-sectional velocity profile as expected inside the potential core. At the larger axial distances the model fits the measurements.

xxx

Figure 23 Description of the cross-sectional velocity profiles

Chapter 7 Power consumption

This research was carried out to examine the effect of an air film around a water jet at the scale of dredging practice at large distances to the nozzle in axial direction. Tests at smaller scales show an increase of the velocities at these positions.

The results of the current research show an increase of the velocities, but this is only observed at relatively small axial distances. The increase of the velocities is observed in a region between x/D_n=6 and x/D_n =36. So at the scale of dredging practice the effect of an air film is less for the applied air discharges.

If an air film is implemented in a practical application an important aspect is the amount of power that is required to create an air film. For the creation of the water jet itself and the air addition a certain amount of power is required, they are defined as P_{water} and P_{air}.

The power to create a water jet is:

$$P_{water} = \Delta p * Q \tag{7.1}$$

with

Δp	=	pressure difference	[Pa]
g	=	gravitational acceleration	[m/s^2]
Q	=	water discharge	[m^3/s]

The power of the air jet is given as:

$$P_{air} = m * c_p * (T_2 - T_1) \tag{7.2}$$

with

m	=	mass flow	[kg/s]
c_p	=	specific heat (1.0)	[kJ/(kg*K)]
T_1	=	reference temperature (288)	[K]
T_2	=	temperature in pressurized condition	[K]

The temperature in pressurized conditions is determined by the isentropic gas relation:

$$\frac{p_2}{p_1} = \left(\frac{T_2}{T_1}\right)^{\frac{k}{k-1}} \tag{7.3}$$

with

p_1	=	reference pressure (atmospheric)	[Pa]
p_2	=	pressure	[Pa]
T_1	=	reference temperature	[K]
T_2	=	temperature in pressurized condition	[K]
k	=	specific heat ratio (1.4)	[-]

The reference temperature is approximately 288 K. This is the temperature measured each day at the start of the test. The reference pressure is the atmospheric pressure.

The efficiency of the pump and compressor are given in Table 20.

Table 20 Efficiencies of a pump and compressor

	efficiency
Pump	± 80%
Compressor	± 30%

In Table 21 the calculated power required for the water jets and to add the air discharges is given.

Table 21 overview of the power required

	Min	Max
p_{jet} [bar]	xxx	xxx
P_w [kW]	xxx	xxx
Q_a [l/s]	10	90
P_a [kW]	0.17	9.9

As seen from Table 21 the energy required to add the air is not more than the energy required creating a water jet.

If a combination of a jet pressure of xxx bar and an air discharge of 68 l/s is used the total amount of energy for this jet is xxx kW (xxx kW+ 3.6 kW).
The extra power of the air addition can also be used for a submerged water jet without an air film, such the amount of power of this jet is xxx kW.

In Figure 24 three different jets are plotted:

- the theoretical line of a submerged water jet without an air film (p_{jet} = xxx bar)
- the measurements of a water jet with air film (jet =xxx bar and $Q_{air;in}$= 68 l/s)
- the theoretical line of a submerged water jet without an air film (p_{jet} = xxx bar)

If the extra power is used to create a jet without an air film the velocities at the centreline of the jet increase, but the increase is larger if the extra power is used for air addition around the water jet.

xxx

Figure 24 Effect of the extra power

Chapter 8 Conclusions & recommendations

In this chapter the conclusions and recommendations of the research are presented.

Conclusions:

- At the scale of dredging practice the effect of an air film around the water jet has also a positive effect on the velocities.
- The increase of the velocities beyond the potential core is observed between 6 and 36 nozzle diameter. No increase of the potential core was observed during the current research. So the effect of the air film is not as expected as described in the hypotheses.
- The range of air discharges tested in the current research is lower than the range of air discharges as given in the hypotheses to obtain a similar effect as in the previous studies on smaller scale jets. The ratios in the current research are small in comparison to the tests carried out by Ginniken et al.
- Depending on the axial distance, the results of the research show the existence of a minimum and optimum air discharge. If the axial distance is small an optimum air discharge exists. The optimum air discharge increases with increasing axial distance. The existence of an optimum air discharge was expected. For large axial distances a minimum amount of air is required to obtain any effect of the air film.
- xxx
- The thickness of the air film is also an indicator of the effect of an air film. The thickness is compared to the disturbances at the surface of the jet and the turbulent length scales in the jet. The effect of an air film is larger if the thickness of the air film is large.
- The measurements can be described according the formulation of Rajaratnam and that of Yahiro and Yoshida. The transition between the two formulations is at the position of $x/D_n=24$. In the region between the potential core and the defined location, the measurements are fitted by Yahiro and Yoshida. Beyond this point the formulation of a submerged water jet according to Rajaratnam is applied. Theoretically this means a translation of the formulation of a submerged water jet over a certain distance. The translation is $11*D_n$ if the case of a jet pressure of xxx bar and an air discharge of 68 l/s is considered.
- The cross-sectional velocity profile inside the potential core is ‘top-hat’-shaped. Beyond the potential core the velocity profiles can be described by a Gaussian distribution.
- xxx
- The extra power of the air addition is less than the power required to create a jet without an air film. The extra power can be used to create a jet without an air film and higher jet pressure, but the increase of the velocities at the centerline is smaller than in case air is added around the jet.

Recommendations:

xxx

References

- Foeht E. (2008) The structure of three-dimensional sheet cavitation, *PhD-thesis*, 3ME, TU Delft, Delft.
- Ginneken R. et. al. (2006). Verbeteren van de stuwdruk van een water jet onder water, *BSc-thesis*, 3ME, TU Delft, Delft .
- McKeogh E.J. and Ervine D.A. (1981) Air entrainment rate and diffusion pattern of plunging liquid jets, *Chemical Engineering Science,* volume 36 p.1161-1172.
- Rajaratnam N. (1976) Turbulent jets*, Elsevier*, Amsterdam
- Rajaratnam N. and Albers C. (1998) Water distribution in very high water jets in air, *Journal of hydraulic engineering,* June 1998 p. 647-65*0.*
- Tennekes H. and Lumley J.L. (1970) A first course in turbulence, *book, MIT Press,* Cambridge.
- Vinke F.R.S. (2009) Water jets surrounded by an air film*; Literature study*; CITG, TU Delft, Delft
- White F.M. (1998) Fluid mechanics, *book, McGraw-Hill Education,* .
- Yahiro T. and Yoshida, H. (1974) On the characteristics of high speed water jet in the liquid and its utilization on induction grouting method*, second international symposium on Jet cutting technology*, Cambridge.

List of Symbols

Variable	description	dimension
A	surface	[m^2]
A_t	surface of the orifice	[m^2]
b	radial position to the centre of the jet, where $u/u_m = 1/2$	[m]
b_w	radial position to the centre of the jet, where $c/c_m = 1/2$	[m]
C_d	dimensionless discharge coefficient	[-]
c_w	water concentration	[%]
c_m	water concentration at the centre axis	[%]
c_p	specific heat	[J/(kg*K)]
d	diameter of the orifice in the orifice plate	[m]
D	diameter of the pipe	[m]
D_j	jet diameter	[m]
D_n	nozzle diameter	[m]
E	velocity approach factor	[-]
F_1, F_2	correlation factors	[-]
g	gravitational acceleration	[m/s^2]
h	distance between top of the bucket and inside water level	[m]
k	specific heat ratio	[-]
L	length of the initial region	[m]
L_t	turbulent length scale in axial direction	[m]
L_f	length where over friction loss is present	[m]
l_t	turbulent length scale in radial direction	[m]
M	momentum	[N]
M	mass of mol (0.288)	[kg/mol]
m	mass flow	[kg/s]
Δp	pressure difference	[Pa]
p	pressure	[Pa]
p_a	atmospheric pressure	[Pa]
p_b	pressure inside the bucket	[Pa]
p_d	dynamic pressure	[Pa]
p_s	static pressure	[Pa]
p_{stag}	stagnant pressure	[Pa]
p_1	reference pressure	[Pa]
p_2	pressure	[Pa]
Q	discharge	[m^3/s]

Q_a	air discharge	[m^3/s]
$Q_{air,in}$	air discharge according to the discharge meter	[m^3/s]
$Q_{air,loss}$	air discharge ascending to the water surface	[m^3/s]
$Q_{air,netto}$	air discharge effectively used for air film	[m^3/s]
Q_e	entrainment discharge	[m^3/s]
Q_0	discharge at nozzle	[m^3/s]
R	gas constant (8.3145)	[J/(K*mol)]
Re	Reynolds number	[-]
r	position in radial direction	[m]
S	Sutherland's constant for gaseous material	[K]
T	temperature	[K]
T_0	reference temperature	[K]
T_1	reference temperature	[K]
T_2	temperature in pressurized condition	[K]
t	air film thickness	[m]
u	velocity	[m/s]
u_m	velocity at the centre axis of the jet	[m/s]
$u_{0;water}$	exit velocity of the water jet	[m/s]
V	volume	[m^3]
V_a	volume of air at atmospheric pressure	[m^3]
V_b	volume in the bucket	[m^3]
We	Weber number	[-]
x	position in axial direction	[m]
z	position to reference level z=0	[m]
α	scaling parameter	[-]
α_f	dimensionless flow coefficient	[-]
β	ratio between duct diameter and orifice diameter d/D	[m]
λ	friction factor	[-]
μ	viscosity at input temperature	[Pa*s]
μ_0	viscosity at reference temperature T_0	[Pa*s]
υ	kinematic viscosity	[m^2/s]
ρ	density of the mixture or medium	[kg/m^3]
σ	surface tension	[N/m]

List of Figures and Tables

Appendix

A Measurement devices: considerations and design

The velocities and air discharge can be measured by use of different types of methods or equipment.

For instance the velocity can be measured by:

- Pitot tube
- EMS (Electromagnetic Flow Meter)
- ADV (Acoustic Doppler Velocimeter)
- LDA (Laser Doppler Anemometry)
- PIV (Particle Image Velocimetry)

The air discharge can be measured by an air discharge meter based on different principles:

- Thermal mass flow
- Vortex flow meter
- Orifice plate
- Flow nozzle

Pitottube
With the pitottube a pressure difference is measured between the static pressure and the pressure due to the velocity (stagnant pressure). The static pressure, P_t, is measured at the side of the tube while the stagnant pressure, P_s, is measured at the tip of the tube at the stagnation point.
The relation between the pressure difference and the velocity is given by:

$$P_t - P_s = \frac{1}{2} * \rho * u^2$$

The pros are the simplicity of the method and the low costs.
In most cases the only medium is water or air, but in these experiments water and are will be used simultaneously. A correction has to be made for the density of the air-water mixture. The pitot tube becomes also inaccurate when the velocities in the flow are low.

Array of conductivity probes
If a pitot tube is used the density of the mixture has to be measured to obtain the velocity. In one-phase flow the density is known, but in two-phase flow the real density of the mixture is unknown. It is possible to obtain the density of the mixture with use of an array of conductivity probes. This apparatus is a tube of 1cm diameter and contains pairs of probes, which measure the conductivity of the medium between the probes.

EMS (electromagnetic flow meter)
The operation of this type of equipment is based on the moving charge in a magnetic field. The moving charge causes a potential difference. This potential difference is proportional to the velocity of the charge carried by the flow. The pros of this method are the easy use of this probe and it can measure two velocity components simultaneously. This device has to be calibrated properly and this device is susceptible for electronic noise and zero-offset drift.

This device measures a certain volume of water, so this is a mean velocity. The sampling volume is several cubic centimeters. Accurate measurements can be done up to a velocity of 5or 6 m/s.

ADV (Acoustic Doppler Velocimeter)
This method determines the velocity by means of ultrasound pulses produces by a transmitter, which are confined to a single beam. The fine particles in the flow will scatter the sound waves and will be detected by receivers. The receivers measure a Doppler shift in the ultra sound frequency caused by the flow. This apparatus measures a three dimensional velocity vector and is used to obtain velocities on very small scales. A good calibration is needed for the speed of sound. The sample volume is smaller than one cubic centimeter.

LDA (Laser Doppler Anemometry)
This apparatus uses the same technique as the ADV, but in this case the deflection of a laser beam is measured. The laser beam is produced by two lasers. With this method a very small probing volume is created to measure the very small fluctuations in the velocities.

PIV (Particle Image Velocimetry)
This method is used by Foeth (2008) in his research. The objectives of the research are to provide a better insight of the physical mechanisms governing the dynamics and structure of a sheet cavity, provide accurate and detailed data of an unsteady cavity on various configurations that can be used for validation of computational models and the last obejective is to interpret the results and to contribute to the development guidelines for propeller design. The objectives give rise to detailed flow measurements of cavitating flow.

PIV is an optical measuring technique for gaseous and liquid flows. The principle of this method is as follows. Small particles are added to the flow and if the size of the particles is not too large and the particles have almost the same density as the fluid, it may be assumed that the particles follow the flow and can be considered as fluid tracer particles: their velocity will be the same as the fluid velocity.
A light sheet is obtained by expanding the laser beam by lenses and this sheet illuminates a slice of the fluid domain, so also the particles in the sheet. The dimensions of the sheet are approximately 200*200mm. Perpendicular to the sheet of light a camera is installed, which captures the location of the particles. Images of 1024*1024 pixels are made by the camera. This camera is a high speed camera.
The displacement of the individual particles can be deduced from their location displacement from frame to frame. When the time between the frames and an image scaling is known the velocity can be derived. The accuracy is within 1%.

To derive the velocities a few steps has to be taken. First an image is divided into smaller interrogation windows, ranging from 16 to 128 pixels; approximately 500 fit in one image. The interrogation windows of the first image are cross-correlated with the interrogations window on the second image. The maximum correlation is tried to be obtained using the displacements of the interrogation window on the second image. A correlation map is obtained based on pixel displacement. At the matching displacement a strong correlation peak is observed on the correlation map. Often more then one correlation peaks can be find on the map and the strongest peak may be false. The results are doubtful which may be deleted in post-processing activities. These activities

are comparison with neighbors, checking its absolute value, or comparison of the correlation peak and its second correlation peak. One important feature is PIV does not match individual particles from one image, but particle patterns.

An error in the measurements occurs with high velocities. This is caused by the fact that a lot of particles leave the interrogation window, the smaller areas of one image, between two images. An interrogation window shift can be applied to the expected particle displacement to keep the particle count relatively constant, is given as a solution for this problem.

The velocity is obtained by dividing the displacement of the particles by time between two images. Also the use of an image deformation map is necessary. This map is the result of a calibration procedure and it takes into account the deformation caused by lens flaws or effects of looking through refracting material (windows) at an oblique angle. Although is tried to place the camera perpendicular to the light sheet, the edges of an image are not perfectly perpendicular to the light sheet. This leads to deformation of the image edges, which can be corrected by a calibration function.

In case two-phase flow is considered some other problems could occur. Some of them will be discussed here:

- The particles do not mix with the vapor in the system causing no measurement of the velocity in the vapor layer and vaporous regions reflect the incident laser light. Strong reflections do overexposure the images near the cavity interface, but also particles out side the light sheet will be illuminated.
- Bubbles and other small nuclei in the flow may be interpreted as particles by the interrogation routine.
- The bubbles could be used as tracers as sufficient bubbles are available, but another problem arises. Stresses exerted on the bubbles cause a deformation of the bubbles. The deformation of a bubble may be interpreted as a motion by the interrogation routine.

The use of fluorescent particles does solve the problem of the reflections. To protect the chip of the camera to the laser light and overcome overexposure, an optical filter in front of the camera can be used.
Two problems will not be solved by the use of fluorescent particles; the diffraction of the light sheet by the cavity still illuminate the particles out side the plane and the particles on their turn illuminate the cavity and the test section. This is recorded as background noise by the camera. The problem of the illumination of the particles outside the plane is solved by use of a very narrow depth of field, placing these particles out of focus. This will lead to a lower possibility of forming a strong correlation peak.

It is not possible to interrogate the cavity, although there is a strong correlation on the image. Accurate predictions of the displacements can not be made.
The reasons are:

- The light from the laser is reflected by the cavity, so the intensity recorded by the camera depends on the direction of illumination. Changes in the cavity outline will lead to changes in the intensity of the reflection causing errors in the correlation.
- It is not possible to derive if the recorded cavitation is in- or outside the sheet of light. Most of the time it is outside the sheet. Calibration is only valid in the measurement plane, so interrogation is nearly always erroneous.

- The predictions of the fluid velocities are not correct if changes in the cavity interface are observed, but no changes in the fluid velocity. An example is smooth and stationary interfaces. This leads to a zero-velocity prediction and strong gradients in the velocity field near the interface, while this is not present in the actual flow.

Foeth states that the cavity has to be removed from the images by use of a form of pre-processing to obtain accurate predictions for the velocities near the cavity interface. The removement of the cavity must be done such the particles will remain unharmed. A clear interface has to be found on the images. A clear interface is not always found, especially in cloud cavitation. The results of Foeth with this type of pre-processing are good.

The experiments of Foeth are done in the tunnel of DUT. The dimensions of the tunnel are 600*297*297 mm (L*W*H). This is a closed system where water is circulated.

Considerations:
For the measurement of the velocity a number of techniques can be used. The best method for the experiments in this research has to be chosen.

A pitot tube and EMS are easy to use and can be mounted on a frame. Some electronic cables have to be connected between the device and the Opto-system, but no other special equipment is necessary.

ADV and LDA are methods to determine the velocities at very small scales. The small scale velocities are not the subject of this research.
In case of LDA it is hardly to use in the laboratory of Boskalis. The lasers have to be placed at one side of the flume, while the detectors at the other side. In the laboratory it is only possible to place some apparatus at one side of the flume.

Although PIV is more accurate it takes a lot of more effort to obtain good results from the measurements. A lot of processing and pre-processing on the images has to be done. Foeth (2008) has used the method to be able to measure the velocities as close as possible to the cavity interface, but he was not able to measure the velocities in the cavity with use of this type of method. On the contrary he is removing the cavity on the images to obtain better predictions of the velocity.
He discussed some problems of the method in a flow containing air and water simultaneously. Some problems could be solved and some of them are not large during his experiments.

In the research of Foeth solutions are indicated to overcome the problems of air when PIV is used to obtain the velocities around a cavity.

In this research some problems will remain and other problems arise.
The air is injected as a film around the jet. Foeth indicated that particles in the core of the jet are not illuminated, because the laser sheet is reflected by the air film.
No particles are observed for the interrogation method to obtain the velocity of the particles.
The velocity close to the air–water interface can be obtained if a clear interface of air and water is present. In case of the experiments in this research a clear air-water interface will not be present. The air film will consist of a cloud of air bubbles. So in the pre-

processing it is hard to remove the cavity. An other problem of removing the cavity on the images no particles will be left, while the whole jet is surrounded by air.

The dimensions of the light sheet are small in comparison with the area we are interest in. The area of interest is in the range of 0 – 2 m. This area is larger than the area captured by a laser sheet. The solution of using a number of laser sheets simultaneously is not an option, while a maneuverable laser is not a simple solution.

Foeth has used a laser and two high speed cameras. This is not easy to arrange and the prices of such devices are very high. The scale of the experiments will lead to the use of a lot of particles. Unfortunately these particles are not cheap leading to an increase of the costs.

Conclusion:
Just a few of the aforementioned methods are easy to install and usable with a few adjustments in a flow of air and water simultaneously. These are the pitot tube and EMS. On the other hand for the pitot tube measurement of the density is necessary.
The operation of ADV and LDA in an air-water flow is not known and the LDA requires the placement of devices at both sides of the flume. In the laboratory of Boskalis just at one side of the flume devices can be placed.
The use PIV does not solve the problems in a flow of air and water with just one device. A number of adjustments have to be made, but it is not known if these adjustments will solve all the problems in the experiment of a water jet surrounded by an air film.
The method to obtain the velocities from the images is also laborious and special pre-processing has to be carried out in case of a water jet surrounded by an air film. Foeth has not used the PIV to measure the velocities in the cavity or air bubbles, but the velocity close to the air-water interface. So it is not possible to obtain the velocities inside the core of the water jet with PIV.

The equipment in the experiments will be the pitot tube and EMS. The density is obtained via the measurement of the conductivity of the mixture. This is carried out with an array of conductivity probes. These devices are mounted on a frame.

Air discharge
Besides the velocities the air discharge is an important parameter in this research. The determination of the air discharge can be done with different methods. A method has to be found to obtain accurate discharge measurements of the air injected into the system.

Discharge meter
The easiest way to measure the air discharge is with a discharge meter. The gas discharge can be measured with a thermal mass flow meter. The air will flow along a heat source. The flow will absorb a certain amount of heat, which is proportional to its mass flow. The heat of the source is absorbed by the molecules in the moving gas leading to a cooling down of the heat source. When the flow rate is increased more molecules will come into contact with the heat source, so more heat is absorbed. The amount of dissipated heat is proportional to the number of molecules of a particular gas (its mass), the thermal characteristics of the gas and its flow characteristics. The mass can be transformed to the volume of gas with help of the gas law. The temperature and pressure of the gas flowing through the meter has to be known to be able to derive the discharge. These devices are very expensive.

Vortex flow meters
Another device to measure the discharge is a vortex flow meter. The principle is behind a small strut vortex shedding will occur. An ultrasonic downstream of the strut is detecting the pattern of the vortices.
When the vortices flow trough the beam, they modulate its carries wave. The number of vortices formed is directly proportional to the flow rate. This is also an expensive device.

Orifice plate
This device consists of a plate with a hole leading to a smaller area through which the fluid can flow. The fluid is forced to converge through the hole. The flow is converged to a maximum at a small distance downstream of the orifice plate. This point is called vena contracta point. This will lead to a change in the velocity and pressure. Downstream of the vena contracta the fluid expands again, leading again to changes in the velocity and pressure. So the plate creates a pressure drop, which is measured by the pressure probes. Bernoulli's principle relates the pressures and velocities. If the velocity increases the pressure will decrease and vice versa.
With the use of the law of conservation of energy it is possible to determine the discharge. A few correction factors have to be used in case of gas. The factors have to fulfil some regulations set up by NEN. The regulations give also the dimensions and angles of the orifice plate to obtain reliable results.
The background is given in White (1998).

One of the key parameters if an orifice is applied, is the parameter β. The parameter is defined as $\beta = \frac{d}{D}$. The parameter D is the diameter of the duct and the parameter d is the diameter of the orifice.

If the Bernoulli and continuity equations are applied an estimate of the pressure change over the orifice plate is obtained.

Continuity:

$$Q = \frac{\pi}{4} D^2 u_1 = \frac{\pi}{4} D_2{}^2 u_2 \tag{A.1}$$

Bernoulli:

$$p_0 = p_1 + \frac{1}{2}\rho u_1^2 = p_2 + \frac{1}{2}\rho u_2^2 \tag{A.2}$$

If u_1 is eliminated, the equations are solved for u_2 in terms of the pressure change $p_1 - p_2$:

$$\frac{Q}{A_2} = u_2 \approx \left[\frac{2(p_1 - p_2)}{\rho(1 - D_2^4 / D^4)} \right]^{1/2} \tag{A.3}$$

In this equation the friction is neglected and the exact vena contracta ratio D_2/d is unknown. Assumed is that $D_2/D \approx \beta$ and then the device is calibrated to fit the relation

$$Q = A_t u_t = C_d A_t \left[\frac{2(p_1 - p_2)/\rho}{1 - \beta^4} \right]^{1/2} \tag{A.4}$$

The subscript t denotes the throat of the orifice plate.

The dimensionless discharge coefficient is C_d accounts for the discrepancies in the approximate analysis.

$$C_d = f(\beta, \mathrm{Re}_D) \tag{A.5}$$

where $\mathrm{Re}_D = \dfrac{u_1 D}{\nu}$

The velocity-approach factor E is given as:

$$E = (1 - \beta^4)^{-1/2} \tag{A.6}$$

The parameters C_d and E together are the dimensionless flow coefficient α_f:

$$\alpha_f = C_d E = \frac{C_d}{(1 - \beta^4)^{1/2}} \tag{A.7}$$

Equation (A.4) can be written in equivalent form:

$$Q = \alpha_f A_t \left[\frac{2(p_1 - p_2)}{\rho} \right]^{1/2} \tag{A.8}$$

The value C_d for an orifice is determined by:

$$C_d = f(\beta) + 91.71\beta^{2.5}\,\mathrm{Re}_D^{-0.75} + \frac{0.09\beta^4}{1-\beta^4}F_1 - 0.0337\beta^3 F_2 \qquad \text{(A.9)}$$

where $f(\beta) = 0.5959 + 0.0312\beta^{2.1} - 0.184\beta^8$

The values of F_1 and F_2 are 0.4333 respectively 0.47 if the pressure is measured at the positions one D in front and D/2 after the orifice plate.

The density is influenced by temperature of the air through the orifice. The density is determined by formula A.12.

Flow nozzle
The flow nozzle has the same effect as the orifice plate, but the pressure difference is less. The nozzle is better shaped then the orifice leading to accurate results. There are two methods to integrate them in the pipe. Between two pipe flanges or welded-in between two pipes. The high pressure is measured one diameter upstream of the nozzle, while the low pressure is measured half a diameter downstream.

Pressure transducers
As explained the pressure difference is created artificially in the pipe in case of an orifice plate or flow nozzle and the pressure difference is found in a very short distance. A pressure difference is found over longer distances by the friction of the pipe on the flow. No artificially plate or other object has to be installed in the pipe. So no regulations for the dimensions of such an object are necessary.

The loss of energy over a pipe with a uniform cross-section and a length L is

$$\Delta p = \lambda * \frac{L_f}{D} * \frac{1}{2} * \rho * u^2 \qquad \text{(A.10)}$$

$\Delta p =$ pressure difference [Pa]
$\lambda =$ friction factor
$L_f =$ length where over friction loss is present [m]
$D =$ diameter of the pipe [m]
$\rho =$ density of the medium [kg/m^3]
$u =$ velocity of the flow [m/s]

A problem is to find a good measure for the resistance of the pipe; the friction factor f. The value of this factor is depending on the Reynolds number; laminar or turbulent.

In the laminar case the friction factor is given by

$$\lambda = \frac{64}{\mathrm{Re}}$$

While in turbulent flow the factor is depending on the roughness at the inner surface of the pipe, k and the Reynolds number.
$\lambda = f(\mathrm{Re}, k)$

From the diagram as a function of the Reynolds number and the roughness ratio of the pipe diameter D over height of the roughness elements k, the friction factor can be obtained.

If air is considered, a problem arises. The air is compressible. Due to the increase of the pressure the temperature increases and the volume decreases.
The volume according to that pressure is determined with use of the gas law:

$$p * V = n * R * T \qquad \text{(A.11)}$$

$p =$ pressure	[Pa]
$V =$ volume according pressure	[m^3]
$R =$ gas constant (8.31)	[J/(K*mol)]
$T =$ temperature	[Kelvin]

The density is determined by:

$$\rho_{air} = \frac{p * M}{R * T} = 3.46 * 10^{-3} \frac{p}{T} \qquad \text{(A.12)}$$

$p =$ pressure	[Pa]
$M =$ mass per mol (0.0288)	[kg/mol]
$R =$ gas constant (8.31)	[J/(K*mol)]
$T =$ temperature	[Kelvin]

To obtain the density the temperature has to be measured. Influence of the temperature on the viscosity can be calculated with the formula of Sutherland:

$$\frac{\mu}{\mu_0} = \left(\frac{T}{T_0}\right)^{3/2} \left(\frac{T_0 + S}{T + S}\right) \qquad \text{(A.13)}$$

$\mu =$ viscosity at input temperature [Pa*s]; $1.71e^{-5}$

$\mu_0 =$ reference viscosity at reference temperature T_0 [Pa*s]

$T =$ input temperature [Kelvin]

T_0 = reference temperature [Kelvin]; 273.15

S = Sutherland's constant for gaseous material in question; 110.4 [Kelvin]

Practical problems are for instance the sensitivity of the pressure transducers. If the sensitivity is weak a very long pipe is needed to obtain a pressure difference that can be measured.

Velocity profile in pipe with pitot tube
The air will flow through a pipe where the velocity profile in the pipe will be measured with a pitot tube. The pressure difference measured by the tube and the density of the air the velocity can be derived; see paragraph about the pitot tube.
By integration of the profile an estimate is found for the discharge.
This method has a few problems concerning construction of such a device. The use of high pressures will cause an overpressure in the pipe in comparison with the atmospheric pressure. The air wants to flow from inside the pipe to the atmosphere. So if there is a leakage in the pipe air will escape leading to errors in the measurement. The weak points are the connection of the pipe and the construction wherein the pitot tube is situated.

Consideration
Due to the amount of the injected air no appropriate device was found by different manufactures. So an own device had to be constructed. All pros and contras of the different methods are taken into account to decide which method would be used. The orifice plate was chosen, because a high pressure drop will be measured and it was easier to construct.

Location
In this research tests will be carried out at the scale of dredging practice. This scale is large in compared in comparison with the dimensions of the tunnel at the university. The development of the jet will be influenced by the walls, top and bottom of the tunnel. At a certain distance the flow is like in a pipe instead of a free jet.
Injected air will be trapped in the system leading to errors as the air is not subtracted out of the system. The air will circulate in the system and leads to errors in the amount of air added to the water jet.

In the flume of Boskalis the jet has more space to develop without any influence of the walls or bottom. Further the injected air has the possibility to rise to the surface and to escape out of the system. A disadvantage is that not all methods for the measurement of the velocity can be installed easily if this flume is used.

B Pictures of the experimental setup

In this appendix an overview of the final design of the different parts of the experimental setup is given.

Figure 25 is a picture of the flume in the laboratory of Boskalis.

Figure 25 Picture of the flume in the laboratory

In Figure 26 the hose at the suction side of the pump is shown. The red arrows give the direction of the flow. The diesel driven pump is located outside the laboratory because of the exhaust gases.

Figure 26 Suction hose

Also the diesel driven compressor was located outside, because of the exhaust gases. Pictures of the diesel driven pump and compressor are given in Figure 27.

(a) (b)

Figure 27 Diesel driven Pump (a) and compressor (b)

From the compressor the air flows via a hose to the pressure vessel. To this pressure vessel the air discharge meter is connected. A picture of the pressure vessel and air discharge meter is given in Figure 28.

Figure 28 Air flow meter and pressure vessel

The water flows from the pressure side of the pump via a hose to the water discharge meter. Figure 29 shows a picture of the water discharge and the special pipe segments. The red arrows show the direction of the water flow.

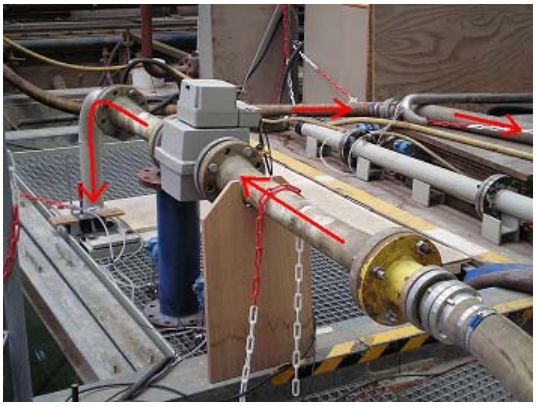

Figure 29 Discharge meter

At the orifice of the nozzle the air is added to the water jet. A picture of the mounted nozzle is given in Figure 30.

Figure 30 Mounted nozzle

Figure 31 show the pictures of the supporting constructions: the fixed water jet construction and the carriage with the measuring probes.

Figure 31 the fixed construction of the water jet (left) and the carriage with measuring probes (right).

The measuring probes are mounted on the measurement frame. Figure 32 shows a picture of the probes mounted on the frame.

Figure 32 Measurement frame

A detail of the fixed water jet construction is given in Figure 33. The picture shows the nozzle, the hose of the air flow and the positions where the water and the air pressure are measured.

Figure 33 Detail of the water jet construction

In Figure 34 a picture of the side view of the carriage is given.

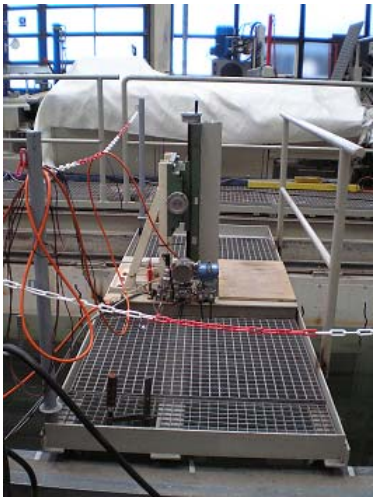

Figure 34 Side view of the carriage

The last figure (see Figure 35) is a picture of the flume if the setup is in operation.

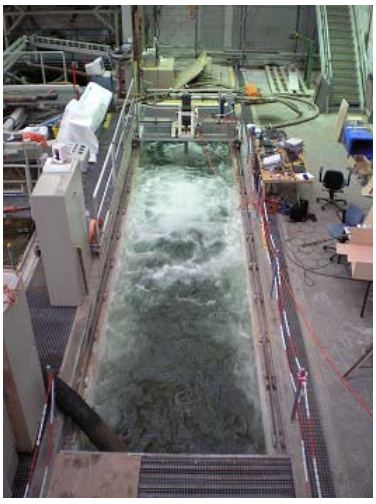

Figure 35 Picture of the flume during the test

C Method of the bucket to determine the net air discharge

During the tests a lot of air was not effectively uses to create an air film around the water jet and so the net amount of air $Q_{air,netot}$, is not equal to the air amount injected according the air discharge meter $Q_{air,in}$. The loss of air was measured by a bucket placed upside down in the flume (see Figure 38). The air that is not used to create the air film is caught in the bucket, leading to an increase of the pressure inside the bucket.

If the system is in rest, the pressure in the bucket equals the atmospheric pressure. When air is injected the air is caught in the bucket and the pressure inside the bucket will increase until a certain level. The water level inside is determined by the pressure. The total volume of air in the bucket can be calculated. If the valve is closed, on top of the bucket (see Figure 39), the pressure increases over a certain time span. So the amount of air inside increases also. The amount of air over time is the discharge lost by the water jet. The different situations of the pressures inside the bucket are shown in Figure 36.

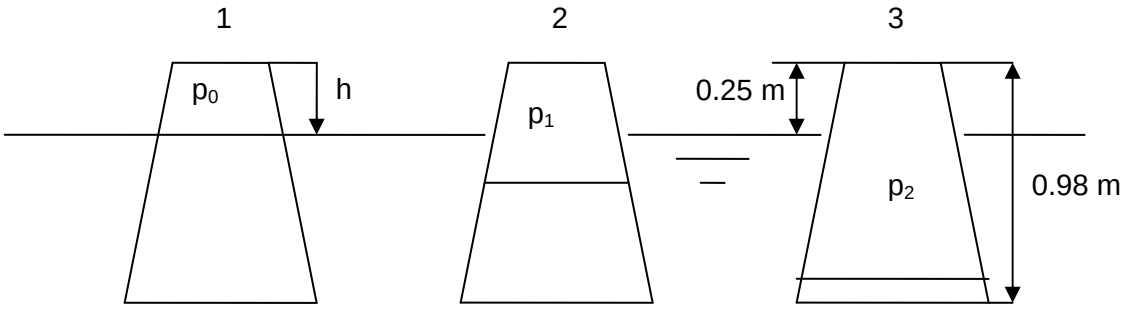

Figure 36 Method of the bucket

1 system in rest; p_0
2 system when air is added and valve is open; p_1
3 system when air is added and valve is closed; p_2

The height of the bucket is 0.98 m. The top of the bucket is positioned 0.25 m above the free water surface.

The pressure inside the bucket is measured as a function of time: dp/dt. The pressure inside the bucket determines the water level inside the bucket.
They are related by $p = \rho g h$.

A schematic figure with the dimensions of the bucket is given in Figure 37.

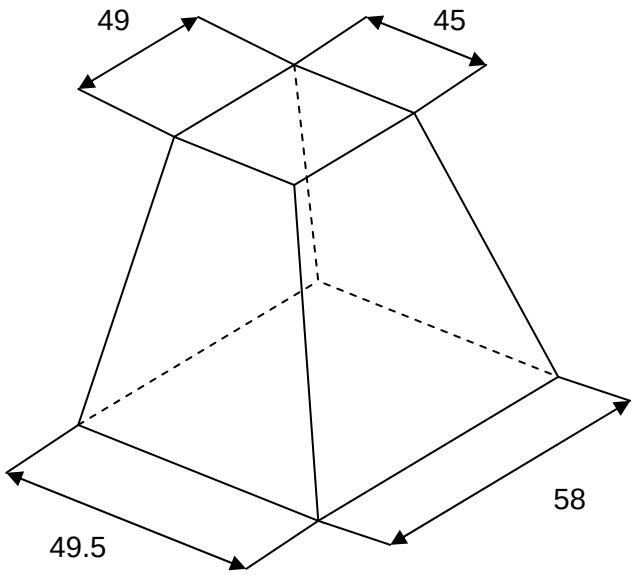

Measures in cm

Figure 37 Schematic figure of the bucket

The volume in the bucket in pressurized condition is:

$$V_b = \int A dh \tag{C.1}$$

with

V_b	=	volume in bucket	[m^3]
A	=	surface of the cross section	[m^2]
h	=	distance between top of the bucket and the water level inside	[m]

A correction is applied to obtain the volume of air in atmospheric conditions:

$$p_b V_b = p_a V_a \tag{C.2}$$

with

V_a	=	volume at atmospheric pressure	[m^3]
V_b	=	volume in bucket	[m^3]
p_a	=	atmospheric pressure	[m^3]
p_b	=	pressure in bucket	[m^3]

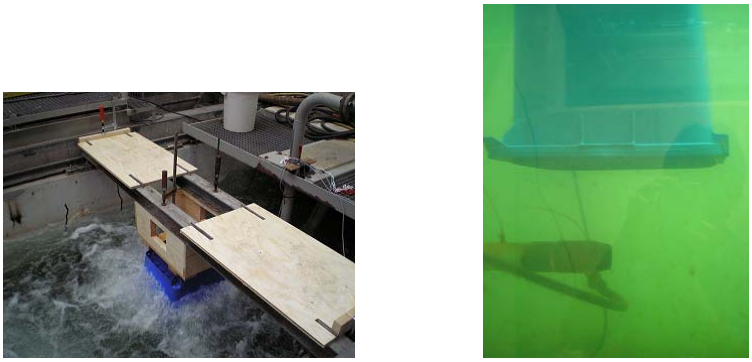

(a) (b)

Figure 38 Photographs of the bucket (a) above water surface (b) submerged

(a) (b)

Figure 39 Picture of the bucket (A) and picture of the valve (B)

D Axes system

The axes system used in this thesis is a Cartesian axes system (right handed) is shown in Figure 40.

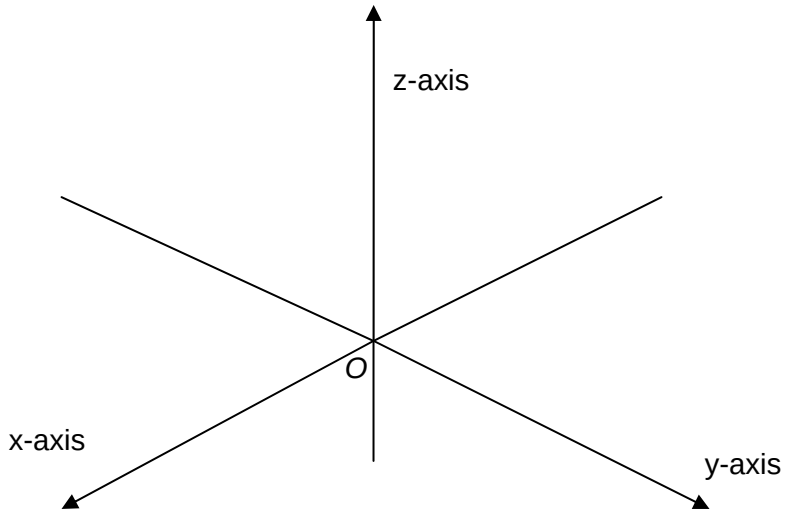

Figure 40 Cartesian axes-system

The origin is lying in the orifice of the nozzle and the x-axis is pointed in the direction of the jet flow. The positive values of the z-axis are situated above the centre axis of the jet, while the position under the axis of the water jet is represented by negative z-values. The region left from the centre axis of the jet is represented by positive y-values. Negative values of y are situated right from the centre axis of the water jet.

E List of signals

During the tests a lot of signals are recorded. They are presented in Table 22. Some corrections had to be made for most of the signals to obtain usable information. The first column of the table contains the parameters, while the second column presents the measurement range of the signal. In the last column the corrections are given.

Table 22 Overview of the signals

Parameter	Range	Correction(s)
Jet pressure:	[0-20 bar, abs.]	$p_{jet} = p_{measurement} + \Delta p_h - p_{atmospheric} + \Delta p_u - \Delta p_{loss}$ $p_{measurement}$ $\Delta p_h = \rho g h$ $p_{atmospheric}$ $\Delta p_u = \frac{1}{2} * \rho * \left(Q / A_{pijp} \right)^2$ $\Delta p_{loss} = \frac{1}{2} * \rho * \lambda * \left(\frac{L}{D} \right) * v^2$ $\Rightarrow \lambda = 0.025$ $\Delta p_{loss} = \frac{1}{2} * \rho * \lambda * \left(\frac{L_1}{D_1} * v_1 + \frac{L_2}{D_2} * v_2 + \frac{L_3}{D_3} * v_3 \right)$
Jet discharge:	[0-40 l/s]	$Q_w = v_{measurement} * A_{pijp}$, $A_{pijp} = \frac{1}{4} * D_{pijp} * \pi$
Air pressure:	[0-7 bar, rel.]	
Air discharge:		
static pressure:	[0-10 bar, rel.]	
Dp over the orifice:	[0-10 kPa, rel.]	
Temperature:	[-25-100 deg. C]	$T_{helvin} = T_m + 273$
(measurement with garbage bin)		
Pitot tube:		
Dp_{pitot}:	[0-10 bar, rel.]	
Staticpressure:	[-1/+1 bar, rel.]	$p_{stat;ptitot;m} + \rho g h - p_{runup}$; $p_{runup} = p_m(t) - p_m(t+1)$
Dynamic pressure:	[0-8 bar, abs.]	$p_{dyn;ptitot;m} - p_{atmospheric} + \rho g h$

EMS	[-5/+5 m/s]	
Conductivity sensors		$Offset = V_{w,m,day} - V_{w,m,validation}$ $\%_{air} = \left[1 - \left[(V_{w,m,d} - (V_{s,m,v} + offset)) * \frac{\%_w - \%_s}{(V_{w,m,v} - V_{s,m})} + \%_s\right]\right] * 100$
Distance	[0-12 m]	$sod_{meters} = x_m - 1.008$ $sod_{dn} = sod_{meters} / D_{jet}$ $D_{jet} = \sqrt{mu} * D_{nozzle}$

F Validation of the conductivity sensors

The validation in case of water and air was carried out by holding all the probes in water or air, while the validation in case of sand was by use of the following method:

Sand is added to the volume of water (see Figure 41). The weight of the sand added to the water is measured in wet condition. A few days later also the weight of the dried sand is measured from different sand samples of the sand added to the water. If the dry weight is known the volume of the dry sand can be calculated:

$$V_{sand,dry} = \frac{W_{s,d}}{\rho_s} \qquad \text{(E.1)}$$

The assumed density is $\rho_s = 2650$ kg/m^3.

After the sand is added the mixture is stirred, causing the mixture to compact to a smaller volume. The volume of the mixture has been measured.

The volume of water and sand in the volume of the mixture is determined by

$$V_{water} = V_{mixture} - V_{sand,dry} \qquad \text{(E.2)}$$

The percentage of water in the sand-water mixture was calculated by

$$\%_w = \frac{V_{water}}{V_{mixture}} \qquad \text{(E.3)}$$

while the percentage of air was calculated by

$$\%_s = \frac{V_{sand,dry}}{V_{mixture}} \qquad \text{(E.4)}$$

As told earlier the sand is dried to obtain the right volume of dry sand added to the water column. This is carried out by putting the sand samples in the oven or put them away in the atmosphere. So from the wet and dry situations it is possible to calculate the percentage of dry sand for the weight as volume of the total weight resp. volume. Numerical calculations are given further on.

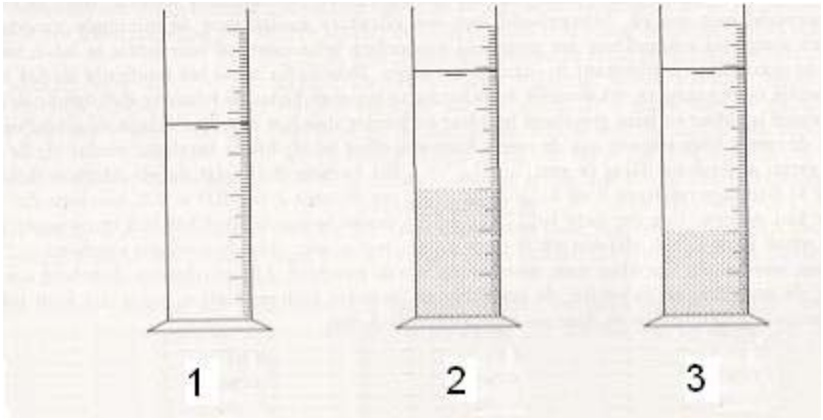

Figure 41 Determination of the porosity

1: water in glass
2: sand has been added
3: situation after stirring

The sensors are validated for water sand and air, but for the calculations only the values of water and sand are used. With all the information a relation between the voltages and sand volumes is given. Between the values of sand and water linear interpolation is used.
During the tests the volume of air is measured instead of sand. The density is calculated by $\%_{water} * \rho_{water} + \%_{air} * \rho_{air}$.

Unfortunately the conditions of the water in the flume changed, so every day a new validation was carried for water. This resulted in an offset per day, but the original slope, voltage and air volume relation, is used.

Validation before the experiments

Table 23 Mass and volumes of the sand samples

Bucket [no.]	$W_{s,wet}$ [gr]	$W_{s,dry}$ [gr]	$V_{s,wet}$ [dm^3]
1	6267	5,34	2,01
2	5977	5,08	1,92
3	6307	5,37	2,03
4	6723	5,73	2,16
5	6905	5,89	2,22
6	6572	5,60	2,11
7	6418	5,46	2,06
8	6292	5,35	2,02
		sum	16.54
	$V_{s,dry}$ [dm^3]		16.54
	$V_{mixture}$ [dm^3]		27.95
	V_{water} [dm^3]		11.42

$$W_{s,dry} = W_{s,wet} * \frac{V_{s,dry}}{V_{s,wet}} \qquad \text{(E.5)}$$

Correction for wet -> dry sand

Table 24 Weight of the sand samples

cup	W_{cup} [gr]	$W_{cup+s,wet}$ [gr]	$W_{s,wet}$ [gr]	$W_{cup+s,dry}$ [gr]	$W_{s,dry}$ [gr]	Factor $\frac{V_{s,dry}}{V_{s,wet}}$
1	3.8	77	73.2	71.4	67,6	0.92
2	3.9	58.3	54.4	54	50,1	0.92
3	3.8	128.3	124.5	100.4	96,6	0.72
					mean	0.87

1) $W_{s,dry} = W_{cup+s,dry} - W_{cup}$

2) $V_{s,wet} = \text{sum}(W_{cup+s,wet}) / \rho_{sand}$

Percentages

$\%_{water} = \frac{V_{water}}{V_{mixture}} * 100$	59.2
$\%_{sand,\,dry} = \frac{V_{sand,dry}}{V_{mixture}} * 100$	40.8

Validation after the experiments

V_0	V_{end}	$V_{m,stirring}$	V_s	V_{winm}	$\%_{water}$	$\%_s$
800	1900	1550	965	584	38	62
800	2000	1550	1052	498	32	68
800	1975	1550	1030	520	34	66

$V_s = (V_{end} - V_0) * 0.88$

$V_{winm} = V_{m,stirring} - V_s$

The outcome of the relation between the percentage of water and the voltages shows a difference between the validation before and after the experiments. The point of sand has shifted to another location while the values of air and water lay on the same place.
To solve this strange phenomenon an extra test is carried out to obtain a good value for the porosity.

Silver sand
Two small sand samples are taken from a bag of sand. The samples are taken from different sides of the bag.

Table 25 Weight and volumes of sand samples (Silver sand, wet)

Sample	W_{cup} [g]	$W_{cup+sand,wet}$ [g]	$W_{sand,wet}$ [g]	$V_{sand,wet}$ [cm^3]
1	5	237.32	232.32	87.66
2	4.98	294.10	289.12	109.10

The sand was put in the oven for two days on a temperature of 105 degrees Celsius

Table 26 Weight and volumes of the sand samples (Silver sand, dry)

Sample	W_{cup} [g]	$W_{cup+sand,dry}$ [g]	$W_{sand,dry}$ [g]	$V_{sand,dry}$ [cm^3]	V_{water} [cm^3]	V_{totaal} [cm^3]
1	5	225.74	220.74	83.29	11.58	94.88
2	4.98	279.51	274.53	103.59	14.59	118.19

The volume of sand of the total volume is 88 %. So from the total volume “sand” added to the water the volume of real sand is 88 % of this volume

Figure 42 shows the relation between voltages and water percentage. The red lines are the calibration before the tests, while the green, blue and purple lines are the calibration when the tests were finished.

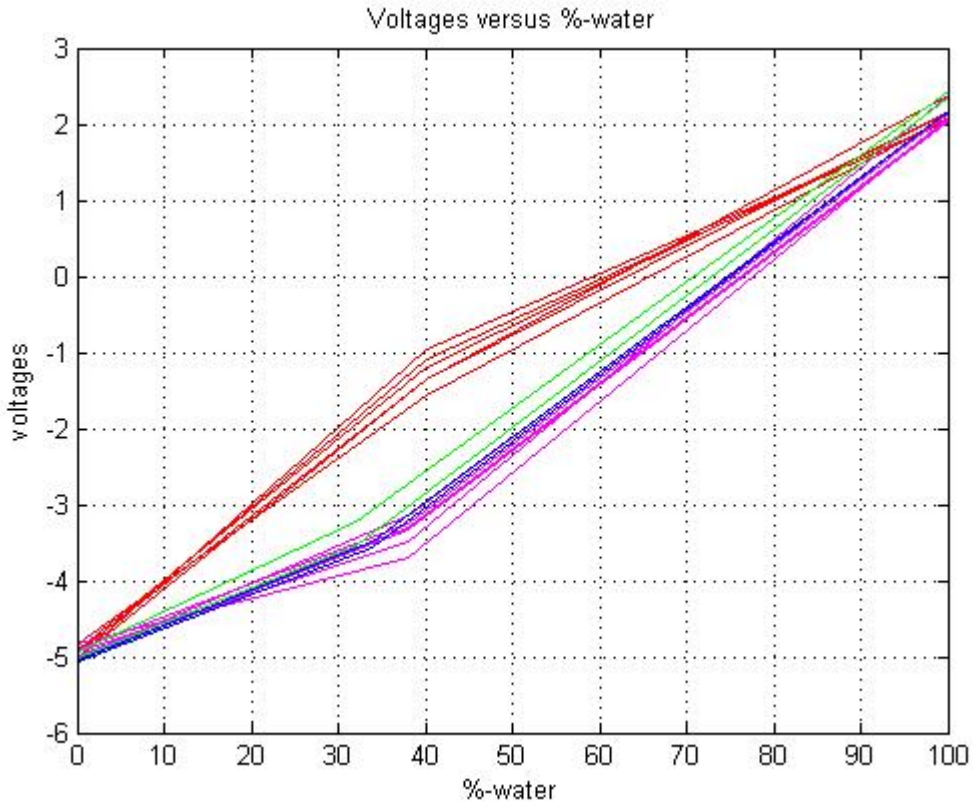

Figure 42 Relation of percentage water and voltages.

A remark is that for the first validation, before the tests, assersand was used and it was dried in a dry room.
After the tests silver sand was taken and it was dried in an oven for two days. This was also carried out for the assersand.

G Technical drawings

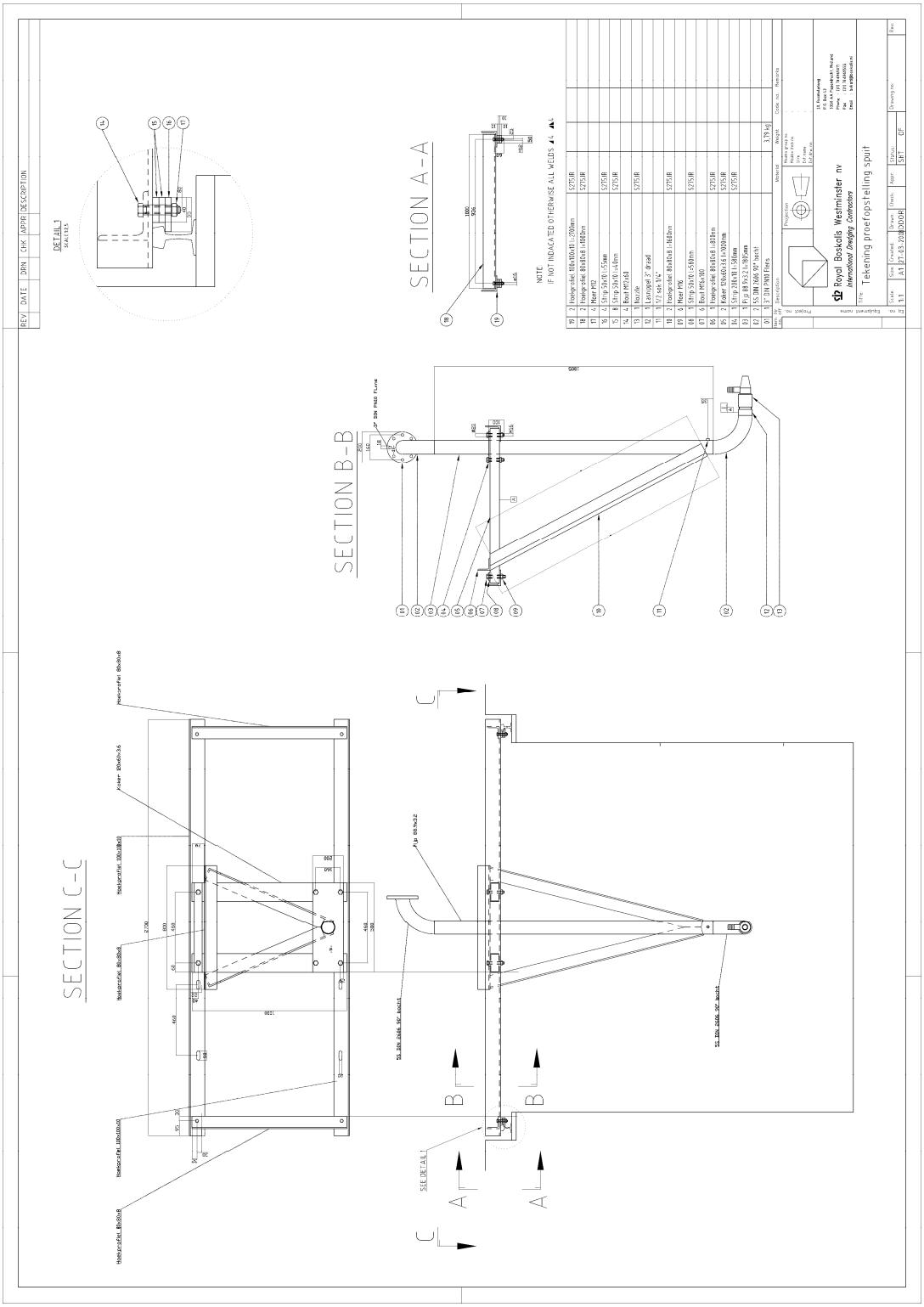

Figure 43 Technical drawing of the support of the water jet

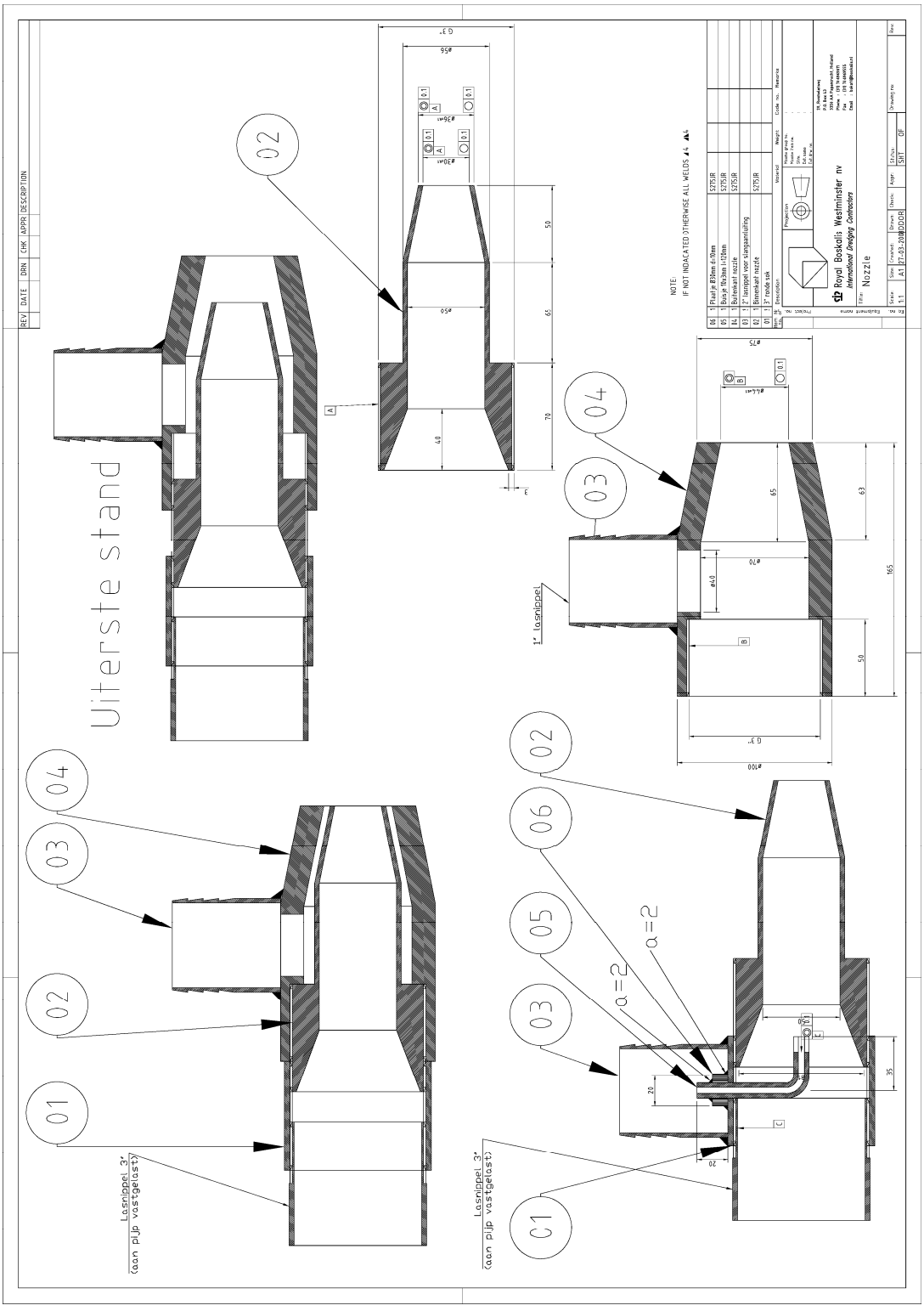

Figure 44 Technical drawing of the nozzle and air chamber

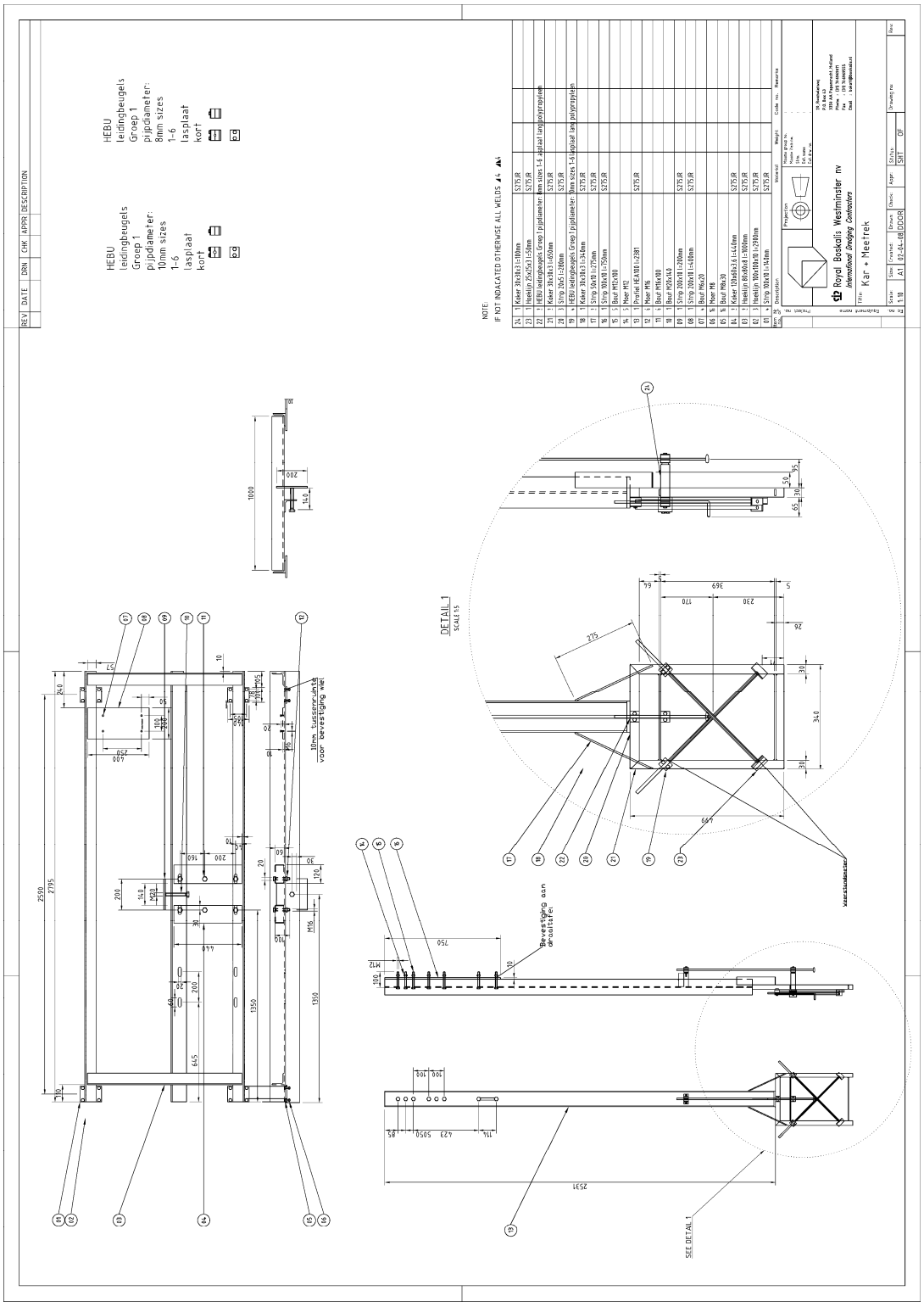

Figure 45 Technical drawing of carriage with measuring probes

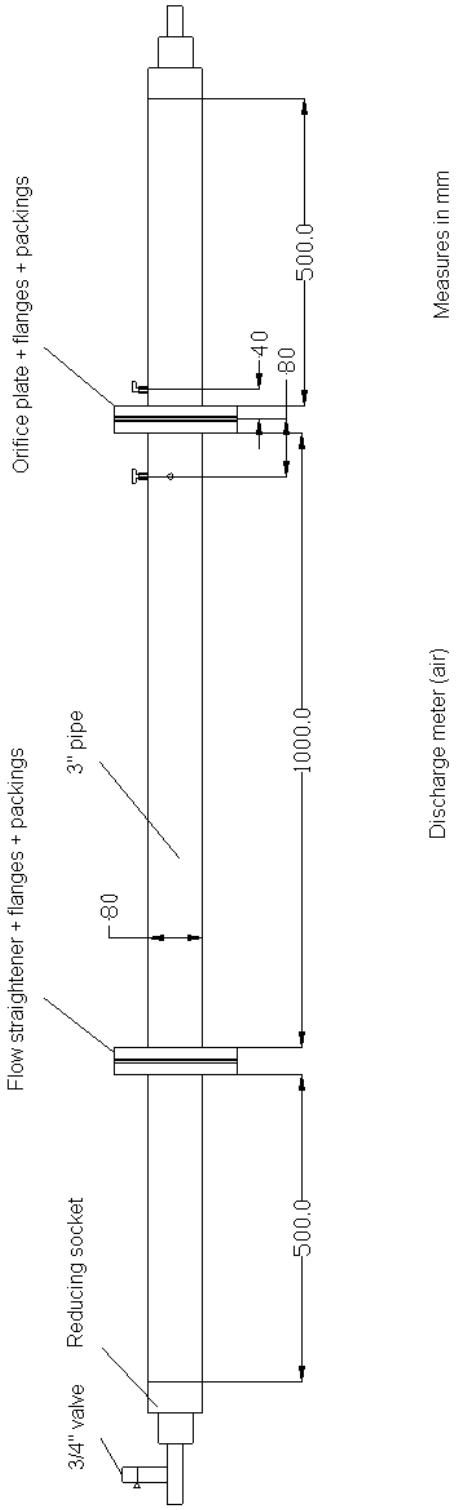

Figure 46 Schematic drawing of the air discharge meter

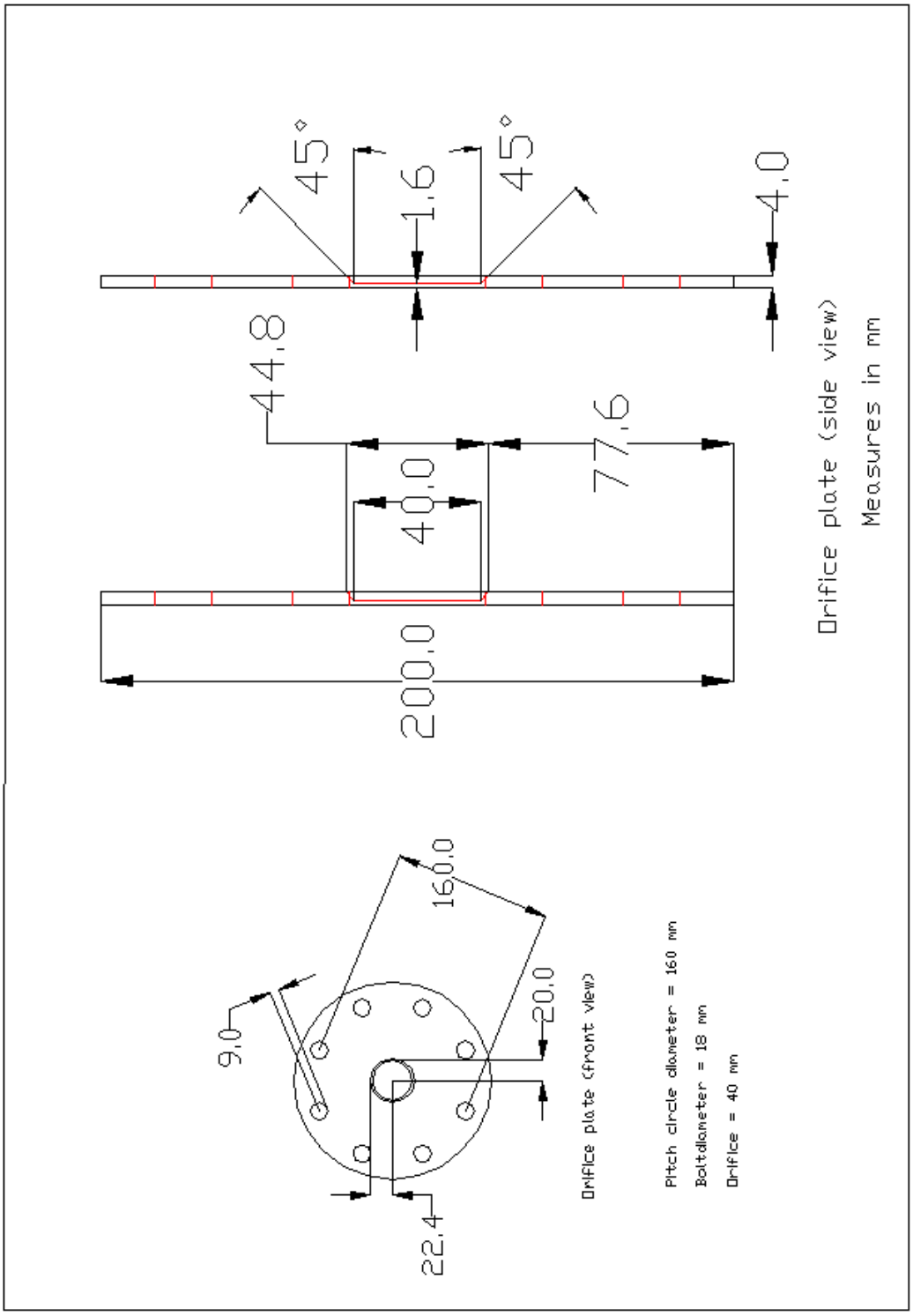

Figure 47 Schematic drawing of the orifice plate

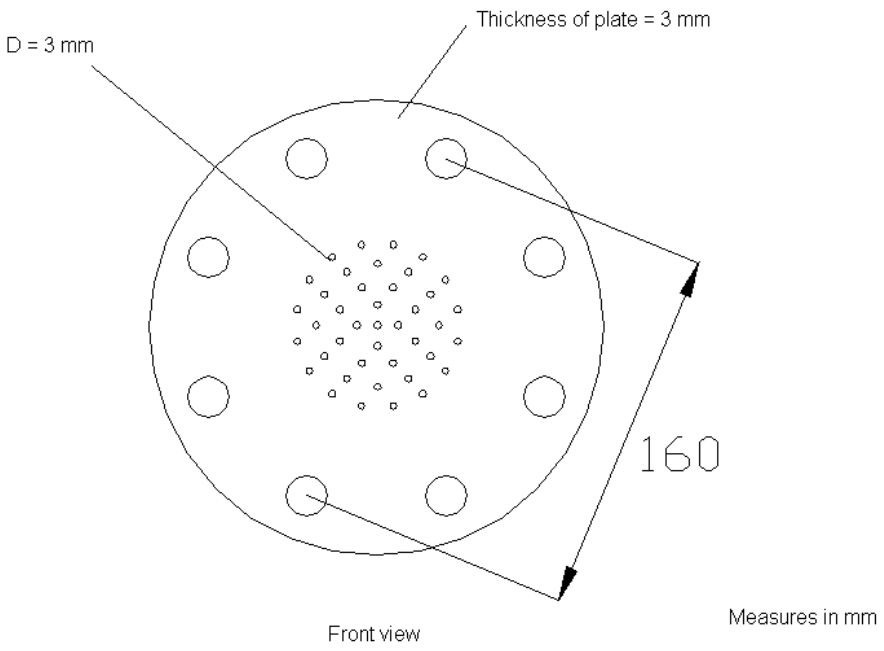

Figure 48 Schematic drawing of the flow straightener

H Figures of a number of jets

In this appendix a number of pictures of the tests are given in Figure 49. The pictures are given for jet pressure between 5 and 8 bar and air discharges 0 and 68 l/s.

$Q_{air;in}$= 0 l/s $Q_{air;in}$= 68 l/s

(A)

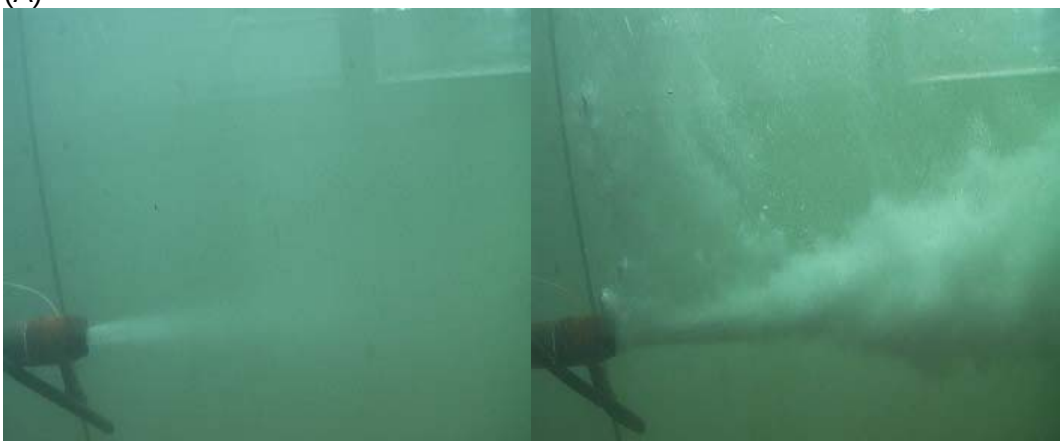

(B)

(C)

$Q_{air;in}$= 0 l/s $Q_{air;in}$= 68 l/s

(D)

Figure 49 Pictures of a number of jets without and with an air film;
(A) p_{jet}=5 bar (B) p_{jet}=6 bar (C) p_{jet}=7 bar (D) p_{jet}=8 bar

J Entrainment of water jets

In chapter 5 the entrainment capacities of a jet are considered. In this appendix the theoretical background is given.

Submerged water jet
According Rajaratnam (1976) the entrainment of a submerged water jet is given by:

$$\frac{Q}{Q_0} = 0.32\frac{x}{D_j} \qquad \text{(J.1)}$$

The discharge is determined at the position SOD=36. As seen from formula (J.1) there is a linear relation between the entrainment and the distance to the nozzle.

Water jet discharging into the atmosphere
Another aspect considered is the air entrainment of a water jet if the water jet is discharging into the atmosphere.
For this type of jet Rajaratnam (1998) describes the development of the cross-sectional velocity profiles at a number of axial distances.
The cross-sectional velocity profile is the profile of the water jet and the air around the water jet.

In the cross-sectional velocity profile a characteristic parameter b is defined. This parameter is the position to the centre of the jet in radial direction where $u = u_m/2$.
The parameter u is the velocity at a position in radial direction to the centre of the jet and the parameter u_m is the velocity at the centre axis. The parameter b increases in axial direction with a growth rate of 0.025. The velocity in radial direction has decreased to a value of approximately zero at a radial distance of five times the parameter b (5*b).

A description of the cross-sectional water concentration profile is also indicated by Rajaratnam. In the cross-sectional water concentration profile a similar parameter as for the cross-sectional velocity profile is defined. The parameter b_w is the position to the centre axis of the jet in radial direction where $c = c_m/2$. The parameter c is the velocity at a position in radial direction to the centre of the jet and the parameter c_m is the velocity at the centre axis.
The growth rate of the parameter b_w in axial direction is 0.005. For distance larger than 600 nozzle diameters the cross-sectional velocity profiles are similar. So for the position SOD=600 the cross-sectional profiles can be sketched both the velocity and the water concentration. Figure 50 shows the values of the different parameters, b and b_w.
A schematic representation of the cross-sectional velocity and water concentration is given in Figure 50.

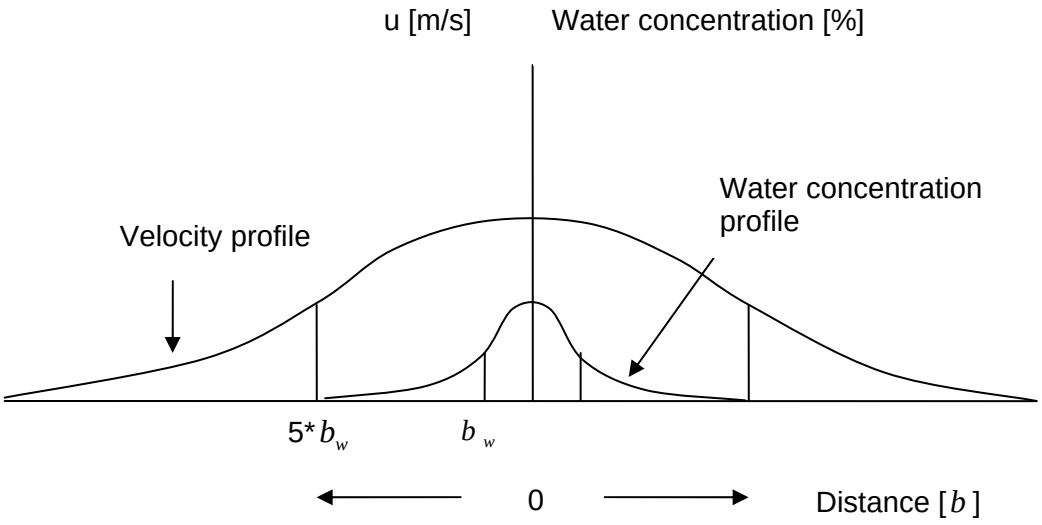

Figure 50 Velocity and water concentration profile at SOD=600.

Table 27 The parameters b and b_w at a distance of 36*D_n

D_n [m]	b [m]	b_w [m]
0.03	0.45	0.09
0.003	0.045	0.009

The velocity profile is given by:

$$u(r) = u_m * \exp^{-0.3*(r^2/b^2)} \qquad \text{(J.2)}$$

with

$u(r)$	=	velocity as a function of the radial position	[m/s]
u_m	=	velocity at the center axis	[m/s]
r	=	radial position	[m]
b	=	characteristic parameter of the width of the velocity profile	[m]

To determine the amount of air entrained by the jet, the velocity profile will be integrated over the distance of the jet width. The jet can be defined if the cross-sectional concentration profile is known.
The cross-sectional water concentration profile is given as:

$$c_w(r) = c_m * \exp^{-0.0055*(r^2/b_w{}^2)} \qquad \text{(J.3)}$$

with

$c_w(r)$	=	water concentration as a function of the radial position	[%]
c_m	=	water concentration at the center axis	[%]
r	=	radial position	[m]

b_w = characteristic parameter of the width of the velocity profile [m]

A visual representation of the cross-sectional water concentration profile is given in Figure 51.

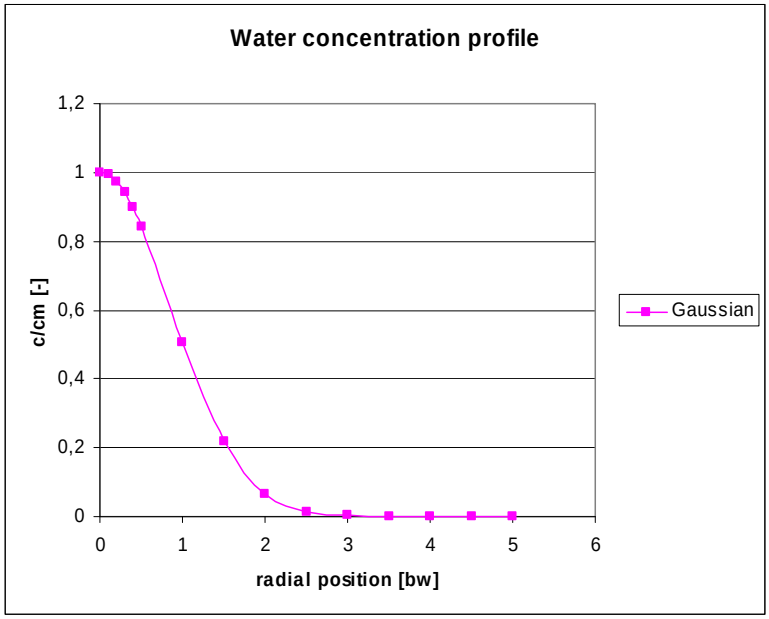

Figure 51 Cross-sectional water concentration profile

The jet is defined as 2.5* b_w. So the amount of air entrained by the water jet over a certain distance can be calculated.

$$Q_e = \int_0^{2.5*b_w} 2\pi r * u(r) * dr - Q_0 \qquad \text{(J.4)}$$

with

Q_e	=	entrained discharge	[m^3/s]
Q_0	=	initial discharge of the water jet	[m^3/s]
$u(r)$	=	velocity as a function of the radial position	[m/s]
r	=	radial position	[m]

Both a profile of the cross-sectional velocities and the water concentration can be calculated at a distance of 600 nozzle diameters.
To determine the entrainment over 36 nozzle diameters the amount of air is assumed to be 36/600 times the entrainment at SOD=600.

The used method is based on several assumptions.

- The water concentration profile at SOD=600 is assumed to be Gaussian.
- The transfer of the entrainment from SOD=600 to SOD=36 is taken linear. This is based on the linear grow of entrainment of a submerged water jet.

K Beaudredge

BeauDredge®

een innovatieve bodemverlagingstechniek

Boskalis bv
Natte en droge infrastructuur

's Gravenweg 399/405
Postbus 4234, 3006 AE Rotterdam
Nederland
Tel: +31 (0)10 - 288 87 77
Fax: +31 (0)10 - 288 87 66
E-mail: n.w.europa@boskalis.nl
Internet: www.boskalisbv.nl

Innovatieve bodemverlaging

BeauDredge® is een nieuwe methode van bodemverlaging die door Boskalis is ontwikkeld. Het gaat hierbij om het realiseren van een bodemverlaging door bruikbaar materiaal (meestal zand) weg te zuigen van onder een laag onbruikbaar materiaal of materiaal waarvan het bijvoorbeeld vanwege flora en/of fauna gewenst is, dat dit blijft liggen.
Het karakter en de samenstelling van de bovenlaag wordt hierbij grotendeels bewaard (Bodem blijft Bodem).
Vrijkomend zand kan gebruikt worden voor de zandhandel of binnen het project voor o.a. de aanleg en het herstel van strandjes en oevers.
In vergelijking met het baggeren van slib kunnen kostbare en ruimtevergende depots achterwege blijven. BeauDredge® kan zowel op land als op water worden toegepast.

BeauDredge® techniek

Het werktuig bestaat uit een meerledig samenstel van buizen, bevestigd aan een ponton of kraan. Het samenstel kan verticaal bewegen en om de langsas roteren. Onderin het roteerbare deel wordt met een horizontaal gerichte waterstraal onder hoge druk het zand losgespoten. Het zand-watermengsel wordt door de binnenbuis opgezogen. Tijdens het proces wordt het volume van het injectiewater en het afgevoerde mengsel exact op elkaar afgestemd, waardoor geen ongewenste stromingen ontstaan.

Toepassingsgebieden

Ecologisch herstel laagveenplassen

Door bodemverlaging wordt een slibvang gecreëerd. De bovenlaag van de put blijft bestaan uit het oorspronkelijke materiaal. Er ontstaat geen extra vervuiling door het weghalen van deze laag.

Aanleg van retentiegebieden

De aanleg van retentiegebieden kan uitgevoerd worden met BeauDredge®. Omdat bodemverlaging wordt gerealiseerd zonder het verwijderen van de bovenlaag, zal het ecologisch evenwicht minimaal worden verstoord.

Rivierverruiming

Voor het project 'Ruimte voor de Rivier' kan BeauDredge® op verschillende manieren toegepast worden:

- uiterwaard verlagen
- nevengeul baggeren
- zomerbed verruimen

Nautisch onderhoud/vaargeulverdieping

Bij het verdiepen van vaarwegen vormt de bovenlaag vaak een probleem.
Deze bestaat dikwijls uit enkele meters (vervuild) slib, veen en/of zachte klei, die niet eenvoudig afgezet of geborgen kan worden. In die gevallen waar zich onder deze laag een zandlaag bevindt, kan BeauDredge® toegepast worden.

Van boven naar beneden:
Prototype proeven Vlijmen; Pilotproject Herfterwetering; Pilotproject Hanzerak-Oost.

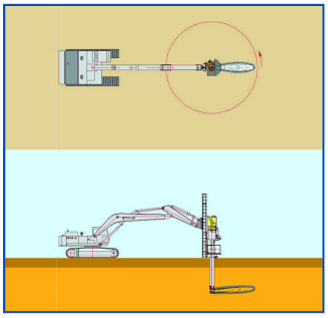

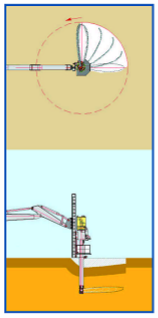

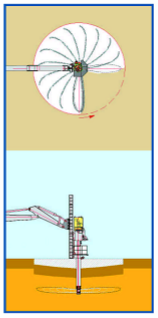

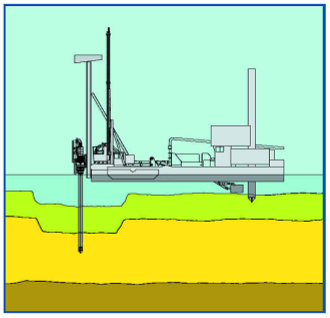

Principe van onderzuigen met BeauDredge®:
Toepassing op het land en op het water.

Pilotproject Hanzerak-Oost.

Verlagen en bezanden van diffuus vervuilde bodems

BeauDredge® kan goed toegepast worden op locaties met diffuus vervuilde bodems, waarbij de methode van bezanden een milieuhygiënisch verantwoorde optie is. Door het afdekken met zand dat lokaal met BeauDredge® is onderzogen, wordt de ruimtelijke verspreiding (opwerveling en stroming) van de vervuilde grond tegengegaan. Afhankelijk van de samendrukbaarheid van de oorspronkelijke deklaag is zelfs netto bodemverlaging mogelijk door het gewicht van het afdekzand.

Overige toepassingsmogelijkheden:

- verdiepen onder woonboten
- ondergraven van wrakken
- selectief ontgronden ten behoeve van o.a. de winning van industriezand

Ervaring met BeauDredge®

Vlijmen: prototype proeven

Om zoveel mogelijk inzicht te krijgen in de verschillende processen is gekozen voor de beproeving van een kleinschalig prototype op het strand van de Boskalis zandwinplas Engelenmeer nabij Vlijmen. De beproeving spitste zich toe op het monitoren van het proces van een aantal cirkelvormige bodemverlagingen. Verschillende procesparameters werden daarbij gehanteerd. Hier werd nog niet de realisatie van een bodemverlagingswerk beproefd. De bevindingen van de prototype beproevingen wezen uit, dat het innovatieve BeauDredge®-concept werkt zoals verwacht.
Met deze bevindingen zijn vervolgens een tweetal pilotproeven verworven teneinde ervaring op te doen met een specifiek werk c.q. specifieke toepassing: pilotproject Herfterwetering en pilotproject Hanzerak-Oost.

Mogelijke schaalvergroting: Twee onderzuigsystemen op een ponton.

Pilotproject Herfterwetering: aanleg van een retentiegebied

Met het doorontwikkelde BeauDredge®-concept is in opdracht van waterschap Groot Salland een deel van een retentiegebied naast de Herfterwetering aangelegd. Naast retentie fungeert deze bodemverlaging tevens als ecologische vernatting conform de inrichtingswens van de gemeente Zwolle.
Een bodemverlaging van ongeveer 0,7 m werd gerealiseerd.
De bovenlaag van de cultuurgrond varieerde van 0,5 m tot 2,0 m.

Pilotproject Hanzerak-Oost: nautische bodemverlaging

In samenwerking met Rijkswaterstaat Directie IJsselmeergebied (RDIJ) is een pilotproject op het Ketelmeer opgestart. Dit project is volledig op het water uitgevoerd. Voor het project Hanzerak-Oost is een geheel nieuw werktuig ontwikkeld en gebouwd.
Het onderzuigwerktuig is bevestigd aan een kraan die op een ponton is geplaatst.

Een bodemverlaging van ongeveer 2 m werd gerealiseerd. De bovenlaag van hoofdzakelijk klei was ongeveer 3 m dik. De oorspronkelijke waterdiepte was 4 m. Voor dit pilotproject is een uitgebreid monitoringsprogramma opgesteld.
De eerste resultaten op het Ketelmeer laten zien dat de vertroebeling in vergelijking met traditionele methodes minimaal is en dat de waterkwaliteit niet beinvloed wordt. Daarnaast is gebleken dat de aanwezige waterbodem zich niet vermengt met het gewonnen zand. Verder is in de nabije polders geen verhoogde kwel geconstateerd.

Toekomst BeauDredge®

BeauDredge® is uitgebreid beproefd, zowel op het land als op het water.
Afhankelijk van de marktwensen zal de BeauDredge® techniek verder worden geoptimaliseerd. Schaalvergroting behoort tot een van de mogelijkheden. Door het toepassen van BeauDredge® wordt het mogelijk om bepaalde projecten te realiseren, die voorheen economisch of technisch niet haalbaar waren.

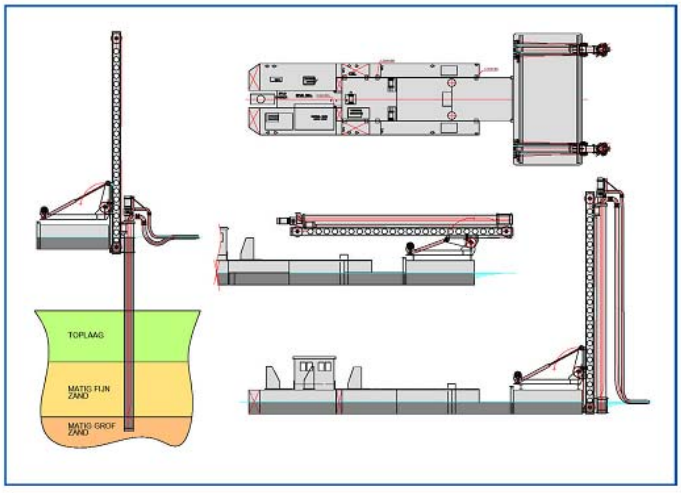

L Opdrachtomschrijving

OVEREENKOMST

Ondergetekenden,

- Baggermaatschappij Boskalis B.V. ten dezen vertegenwoordigd door Ir. A.J. Nobel,

- Het opleidingsinstituut, TU Delft, ten dezen vertegenwoordigd door Prof. Dr. Ir. C. van Rhee en

- De Student, F.R.S. Vinke

hierna te noemen “Partijen”

In aanmerking nemende dat

- Partijen zijn overeengekomen dat de Student een afstudeeropdracht, inclusief het te maken verslag, in een geschatte tijd van 9 maanden uitvoeren.

- De Student werkzaamheden verricht of zal gaan verrichten voor de afstudeeropdracht en daaruit informatie zal ontvangen of op andere wijze daarvan zal (kunnen) kennisnemen (hierna te noemen “de Informatie”). De Informatie omvat onder andere gegevens over werktuigen, uitvindingen, octrooiaanvragen, tekeningen, contracten, opdrachtgevers, leveranciers, afnemers.

- Baggermaatschappij Boskalis actief is op de zandwinningmarkt met behulp van cutterzuigers en sleephopperzuigers.

- Opdrachtomschrijving
Titel: Eigenschappen van een waterjet ondersteund door lucht.

Bij verschillende baggertechnieken wordt gebruik gemaakt van waterjets voor het losmaken van grond. Bij veel toepassingen is de losmaakproductie van de waterjet het belangrijkste criterium. Deze losmaakproductie wordt bepaald door de hoeveelheid impuls. Bij sommige toepassingen, o.a. het selectief baggeren (BeauDredge), is naast de losmaakproductie de indringdiepte een belangrijke factor.
Bij BeauDredge wordt grond losgemaakt door middel van een langzaam roterende waterjet in het horizontale vlak. Door een grotere indringdiepte neemt de hoeveelheid zand dat per cyclus (1 omw.) kan worden weggehaald aanzienlijk toe.
De indringdiepte is afhankelijk van de stroomsnelheid en deze neemt snel af door het feit dat de jet weerstand ondervindt van zijn omgevingswater en water aanzuigt (entrainment) en grond erodeert. De stroomsnelheid is op een bepaalde afstand te laag om nieuwe grond te kunnen eroderen.

Uit proeven (2006) is gebleken dat door het toevoegen van lucht de weerstand die de waterjet ondervindt kan worden gereduceerd. Hierdoor zal de stroomsnelheid ook minder afnemen en de waterjet zal theoretisch gezien een grotere indringdiepte hebben. Er zijn twee mogelijkheden om lucht toe te voegen. Toevoegen van lucht in het hart van de waterjet en als een film om de waterjet heen.

Door het creëren van een film van lucht om de waterjet zal de uittreesnelheid (u_0) tot over een grotere lengte intact blijven. Uit de proeven (2006) is gebleken dat dit geldt in het hart van de waterjet, tot lengtes 36 maal de nozzlediameter. Bij een normale waterjet is dit ongeveer 6 maal de nozzlediameter. De proeven zijn echter op zeer kleine schaal uitgevoerd met een nozzlediameter van 3 mm. De vraag is of het zelfde effect bereikt kan worden met grotere nozzlediameters en/of het extra benodigde vermogen niet te groot wordt.

Hoewel de verwachtingen hoger liggen bij een waterjet omhuld door een film van lucht, zal er toch voor beide methoden experimenten worden uitgevoerd. Dit wordt gedaan om ook het effect van het toevoegen van lucht in het hart van het centrum te kunnen bekijken. Het zwaartepunt van het onderzoek zal hierdoor op de waterjet omhuld met een film van lucht liggen.

In de bovenstaande de proeven (2006) is de invloed van het erosieproces van de grond op de eigenschappen van de waterjet buiten beschouwing gelaten. Hoewel het in praktijk toch van invloed is op de eigenschappen van de waterjet, zal die invloed ook in dit afstudeeronderzoek niet worden meegenomen.

De hoofddoelen van het onderzoek kunnen als volgt worden gedefinieerd:

1. Vaststellen van het snelheidsprofiel van een horizontale waterjet ondersteund door lucht, bij verschillende luchtdebieten en jetdrukken.
2. Opzetten van een eenvoudige modellering om de stroomsnelheid van een waterjet ondersteund met lucht te kunnen voorspellen.

In dit afstudeeronderzoek zal worden geprobeerd om met behulp van de volgende onderzoeksvragen de doelen te bereiken:

- Wat is het minimale debiet om een film rond de waterjet te krijgen?
- Wat is het optimale luchtdebiet (snelheid/dikte van de film) dat moet worden toegevoegd?
- Over welke lengte beïnvloedt de film van lucht het snelheidsprofiel?
- Wat is de invloed van de nozzlediameter op de indringdiepte?
- Wordt de lengte van de film lucht, indringdiepte, groter in zout water?
- Hoeveel vermogen kost het om de lucht toe te voegen en is dit niet te groot?

<u>Op basis van voorgaande verklaren Partijen te zijn overeengekomen dat</u>

1. De volgende werkwijze is voorzien:
   - Het uitvoeren van een literatuurstudie naar het functioneren/eigenschappen van een waterjet in lucht of water.
   - Hypothesen opstellen voor de proeven naar aanleiding van de gelezen literatuur.
   - Het ontwerpen en bouwen van een meetopstelling voor de proeven. Er zal gekeken worden naar benodigde pomp, benodigde luchtcompressor, keuze meetsysteem, ontwerp meetframe, ontwerp leidinglay-out, etc.
   - Uitvoeren van experimenten in het laboratorium van Boskalis. Tijdens de proeven zal het snelheidsprofiel op verschillende afstanden vanaf de nozzle worden gemeten van een horizontale, normale waterjet (referentie) en een jet ondersteund door lucht. De volgende parameters zullen worden gevarieerd: luchtdebiet, jetdruk en aanzuiglengte.
   - Uitwerken en analyseren van de data van de proeven en het verifiëren van de opgestelde hypothesen uit punt 3.
   - Het opstellen van een eenvoudige modellering waarin de invloed van diverse parameters op het snelheidsprofiel, en dus de indringdiepte, naar voren komt. De volgende parameters worden meegenomen in het model:, nozzlediameter, zoet/zout, omgevingsdruk, luchtdebiet en jetdruk. De laatste twee parameters zullen met behulp van de experimenten worden geverifieerd. Tevens moet de eenvoudige modellering het snelheidsprofiel kunnen voorspellen.
   - Bundelen en rapporteren van alle bevindingen uit de bovengenoemde punten.

2. Begeleiding, planning en rapportage

De directe begeleider tijdens deze opdracht is ir. A.J. Nobel, medewerker bij Boskalis. De begeleider binnen TU Delft is dr. Ir. A.M. Talmon. De student is verantwoordelijk voor de voortgang van het project. De begeleiders controleren de voortgang. Gestreefd zal worden naar een tijdbesteding van 40 uur per week, inclusief de rapportage. De opdracht vangt aan op 03-01-2008.

3. Rapportage, archivering en geheimhouding

Alle informatie die door Boskalis als vertrouwelijk aan de student ter beschikking is gesteld dient vertrouwelijk te worden behandeld. De student verbindt zich tot geheimhouding van alle informatie.

De informatie dient op het moment dat de werkzaamheden van de student voor de afstudeeropdracht zijn geëindigd weer te worden teruggegeven aan Boskalis. De informatie mag niet worden gekopieerd en/of aan anderen ter inzage worden gegeven en/of op enigerlei andere wijze aangewend worden dan voorzien in deze overeenkomst, zonder voorafgaande schriftelijke toestemming van Boskalis. Ontwikkelingen en ontwerpen in het kader van de afstudeeropdracht zullen gedurende een periode van twee jaar (na afloop van de afstudeeropdracht) als vertrouwelijk worden beschouwd en zullen niet worden verstrekt aan derden, zonder schriftelijke toestemming van Boskalis. Op gemotiveerd verzoek van Boskalis kan deze geheimhoudingsperiode, voor het beëindigen van de werkzaamheden voor de afstudeeropdracht, worden verlengd met een nader af te spreken periode. Indien er gepubliceerd wordt is dit een coproductie van de TU Delft en Boskalis. Hierbij worden de auteurs vermeld.

Er zullen uiteindelijk twee versies van het verslag worden gemaakt:

Versie 1 (vertrouwelijk):
Volledige rapportage voor Boskalis, die alle originelen behoudt. Deze versie is alleen bestemd voor Boskalis en de leden van de examencommissie. De voorzitter van de examencommissie van de te begeleiden student ontvangt één originele versie om te behouden teneinde aan zijn functionele verplichtingen, gesteld bij of krachtens de wet en/of voorschriften van de TU Delft, te kunnen voldoen. De voorzitter van de examencommissie zal deze originele versie als vertrouwelijk behandelen. Beoordeling van de afstudeeropdracht is gebaseerd op deze volledige versie. Vermenigvuldiging en distributie van versie 1 wordt gedaan door Boskalis.

Versie 2 (voor derden):
De versie voor de student en de TU Delft. Het betreft een ingekorte versie 1, zonder vertrouwelijke informatie, goedgekeurd door Boskalis. Boskalis houdt twee van deze kopieën. Vermenigvuldiging en distributie van versie 2 wordt verzorgd door de student.

4. Eventuele octrooien

Uitvindingen
Voor zover nodig en voorzover rechten op uitvindingen al niet van rechtswege aan Boskalis toekomen, draagt de student alle rechten op uitvindingen, daaronder ook begrepen die rechten welke niet vatbaar zijn voor octrooi, reeds nu voor alsdan aan Boskalis over, althans zal hij een dergelijk recht, zodra dat is ontstaan, op eerste verzoek overdragen aan Boskalis.

Boskalis zal uit het onderzoek voortkomende kennis en ervaringen, mits commercieel interessant, middels het aanvragen van octrooien, patenten en het vestigen van intellectuele eigendomsrechten tegen onbevoegd gebruik door derden beschermen. Bedoelde octrooien c.q. patenten zullen ten name van Boskalis worden gesteld, met vermelding van de echte uitvinder(s)

als uitvinder(s). De kosten hiervoor zullen door Boskalis worden gedragen. Indien de TU Delft een octrooi wil aanvragen en Boskalis dit niet commercieel interessant acht, dan mag de TU Delft dit doen voor eigen rekening en met een onherroepelijke, onbeperkte en kostenloze licentie voor Boskalis.

Aansprakelijkheid
De student erkent en aanvaardt dat, in geval van schending door hem van enige verplichting uit hoofde van deze overeenkomst, Boskalis hem in rechte of anderszins zal kunnen aanspreken.

De student,	De hoogleraar van de TU Delft,	Namens Boskalis,
……..	…….	…….
F.R.S. Vinke	Prof. Dr. Ir. C. van Rhee	Ir. A.J. Nobel
datum:	datum:	datum: